

*ARMY RESEARCH LABORATORY*



## **A Solution of the Alekseevski-Tate Penetration Equations**

**by William Walters and Cyril Williams**

**ARL-TR-3606**

**September 2005**

## **NOTICES**

### **Disclaimers**

The findings in this report are not to be construed as an official Department of the Army position unless so designated by other authorized documents.

Citation of manufacturer's or trade names does not constitute an official endorsement or approval of the use thereof.

Destroy this report when it is no longer needed. Do not return it to the originator.

# **Army Research Laboratory**

Aberdeen Proving Ground, MD 21005-5066

---

---

**ARL-TR-3606**

**September 2005**

---

---

## **A Solution of the Alekseevski-Tate Penetration Equations**

**William Walters and Cyril Williams**  
**Weapons and Materials Research Directorate, ARL**

<b>REPORT DOCUMENTATION PAGE</b>			<i>Form Approved</i> <i>OMB No. 0704-0188</i>	
Public reporting burden for this collection of information is estimated to average 1 hour per response, including the time for reviewing instructions, searching existing data sources, gathering and maintaining the data needed, and completing and reviewing the collection information. Send comments regarding this burden estimate or any other aspect of this collection of information, including suggestions for reducing the burden, to Department of Defense, Washington Headquarters Services, Directorate for Information Operations and Reports (0704-0188), 1215 Jefferson Davis Highway, Suite 1204, Arlington, VA 22202-4302. Respondents should be aware that notwithstanding any other provision of law, no person shall be subject to any penalty for failing to comply with a collection of information if it does not display a currently valid OMB control number. <b>PLEASE DO NOT RETURN YOUR FORM TO THE ABOVE ADDRESS.</b>				
<b>1. REPORT DATE (DD-MM-YYYY)</b> September 2005		<b>2. REPORT TYPE</b> Final		<b>3. DATES COVERED (From - To)</b> September 2004–July 2005
<b>4. TITLE AND SUBTITLE</b> A Solution of the Alekseevski-Tate Penetration Equations			<b>5a. CONTRACT NUMBER</b>	
			<b>5b. GRANT NUMBER</b>	
			<b>5c. PROGRAM ELEMENT NUMBER</b>	
<b>6. AUTHOR(S)</b> William Walters and Cyril Williams			<b>5d. PROJECT NUMBER</b> AH80	
			<b>5e. TASK NUMBER</b>	
			<b>5f. WORK UNIT NUMBER</b>	
<b>7. PERFORMING ORGANIZATION NAME(S) AND ADDRESS(ES)</b> U.S. Army Research Laboratory ATTN: AMSRD-ARL-WM-TC Aberdeen Proving Ground, MD 21005-5066			<b>8. PERFORMING ORGANIZATION REPORT NUMBER</b> ARL-TR-3606	
<b>9. SPONSORING/MONITORING AGENCY NAME(S) AND ADDRESS(ES)</b>			<b>10. SPONSOR/MONITOR'S ACRONYM(S)</b>	
			<b>11. SPONSOR/MONITOR'S REPORT NUMBER(S)</b>	
<b>12. DISTRIBUTION/AVAILABILITY STATEMENT</b> Approved for public release; distribution is unlimited.				
<b>13. SUPPLEMENTARY NOTES</b>				
<b>14. ABSTRACT</b> The Alekseevski-Tate equations have been used for five decades to predict the penetration, penetration velocity, rod velocity, and rod length of long-rod penetrators and similar projectiles. These nonlinear equations were originally solved numerically and more recently by the exact analytical solution of Walters and Segletes. However, due to the nonlinear nature of the equations, penetration was obtained implicitly as a function of time. The current report obtains the velocities, length, and penetration as an explicit function of time by employing a perturbation solution of the nondimensional Alekseevski-Tate equations. Explicit analytical solutions are advantageous in that they clearly reveal the interplay of the various parameters on the solution of the equations. Perturbation solutions of these equations were first undertaken by Forrestal et al., up to the first order, and good agreement with the exact solutions was shown for relatively short times. The current study obtains a third-order perturbation solution and includes both penetrator and target strength terms. This report compares the exact solution to the perturbation solution, and a typical comparison between the exact and approximate solution for a tungsten rod impacting a steel armor target is shown. Also, alternate ways are investigated to normalize the governing equations in order to obtain an optimum perturbation parameter. In most cases, the third-order perturbation solution shows near perfect agreement with the exact solutions of the Alekseevski-Tate equations. This report compares the exact solution to the perturbation solution, and comments are made regarding the range of validity of the explicit solution.				
<b>15. SUBJECT TERMS</b> penetration, Tate equations, perturbation theory				
<b>16. SECURITY CLASSIFICATION OF:</b>			<b>17. LIMITATION OF ABSTRACT</b>  UL	<b>18. NUMBER OF PAGES</b>  50
<b>a. REPORT</b> UNCLASSIFIED	<b>b. ABSTRACT</b> UNCLASSIFIED	<b>c. THIS PAGE</b> UNCLASSIFIED		
				<b>19b. TELEPHONE NUMBER (Include area code)</b> 410 278-6062

---

## Contents

---

<b>List of Figures</b>	<b>iv</b>
<b>List of Tables</b>	<b>vi</b>
<b>Acknowledgments</b>	<b>vii</b>
<b>1. Introduction</b>	<b>1</b>
<b>2. Parametric Studies</b>	<b>11</b>
<b>3. Conclusions</b>	<b>29</b>
<b>4. References</b>	<b>30</b>
<b>Appendix. FORTRAN Computer Program</b>	<b>31</b>
<b>Distribution List</b>	<b>36</b>

---

## List of Figures

---

Figure 1. Comparison between rod and penetration velocities for a first-order perturbation solution, a third-order perturbation solution, and the exact Tate solution. This case is for a tungsten rod impacting a steel target at an impact velocity of 2000 m/s. The initial rod length was 0.500 m. ....	6
Figure 2. Penetration depth for a first-order perturbation solution, a third-order perturbation solution, and the exact Tate solution. This case is for a tungsten rod impacting a steel target at an impact velocity of 2000 m/s. The initial rod length was 0.500 m. ....	7
Figure 3. Rod length for a first-order perturbation solution, a third-order perturbation solution, and the exact Tate solution. This case is for a tungsten rod impacting a steel target at an impact velocity of 2000 m/s. The initial rod length was 0.500 m. ....	8
Figure 4. Comparison between rod and penetration velocities for a first-order perturbation solution, a third-order perturbation solution, and the exact Tate solution. This case is for a tungsten rod impacting a 25-mm-thick steel target at an impact velocity of 2000 m/s. The initial rod length was 0.03912 m. ....	9
Figure 5. Penetration depth for a first-order perturbation solution, a third-order perturbation solution, and the exact Tate solution. This case is for a tungsten rod impacting a 25-mm-thick steel target at an impact velocity of 2000 m/s. The initial rod length was 0.03912 m. ....	10
Figure 6. Rod length for a first-order perturbation solution, a third-order perturbation solution, and the exact Tate solution. This case is for a tungsten rod impacting a 25-mm-thick steel target at an impact velocity of 2000 m/s. The initial rod length was 0.03912 m. ....	11
Figure 7. Comparison between rod and penetration velocities for a first-order perturbation solution, a third-order perturbation solution, and the exact Tate solution. This case is for a tungsten rod impacting a steel target at an impact velocity of 3000 m/s. The initial rod length was 0.500 m. ....	12
Figure 8. Penetration depth for a first-order perturbation solution, a third-order perturbation solution, and the exact Tate solution. This case is for a tungsten rod impacting a steel target at an impact velocity of 3000 m/s. The initial rod length was 0.500 m. ....	13
Figure 9. Rod length for a first-order perturbation solution, a third-order perturbation solution, and the exact Tate solution. This case is for a tungsten rod impacting a steel target at an impact velocity of 3000 m/s. The initial rod length was 0.500 m. ....	14
Figure 10. Comparison between rod and penetration velocities for a first-order perturbation solution, a third-order perturbation solution, and the exact Tate solution. This case is for a steel rod impacting a silica-sand target at an impact velocity of 3000 m/s. The initial rod length was 0.03912 m. ....	15
Figure 11. Penetration depth for a first-order perturbation solution, a third-order perturbation solution, and the exact Tate solution. This case is for a steel rod impacting a silica-sand target at an impact velocity of 3000 m/s. The initial rod length was 0.03912 m. ....	16

Figure 12. Rod length for a first-order perturbation solution, a third-order perturbation solution, and the exact Tate solution. This case is for a steel rod impacting a silica-sand target at an impact velocity of 3000 m/s. The initial rod length was 0.03912 m.....	17
Figure 13. Comparison between rod and penetration velocities for a first-order perturbation solution, a third-order perturbation solution, and the exact Tate solution. This case is for a 93% tungsten rod impacting a steel target at an impact velocity of 2000 m/s. The initial rod length was 0.500 m.....	18
Figure 14. Penetration depth for a first-order perturbation solution, a third-order perturbation solution, and the exact Tate solution. This case is for a 93% tungsten rod impacting a steel target at an impact velocity of 2000 m/s. The initial rod length was 0.500 m.....	19
Figure 15. Rod length for a first-order perturbation solution, a third-order perturbation solution, and the exact Tate solution. This case is for a 93% tungsten rod impacting a steel target at an impact velocity of 2000 m/s. The initial rod length was 0.500 m.....	20
Figure 16. Comparison between rod and penetration velocities for a first-order perturbation solution, a third-order perturbation solution, and the exact Tate solution. This case is for a 93% tungsten rod impacting a steel target at an impact velocity of 3000 m/s. The initial rod length was 0.500 m.....	21
Figure 17. Penetration depth for a first-order perturbation solution, a third-order perturbation solution, and the exact Tate solution. This case is for a 93% tungsten rod impacting a steel target at an impact velocity of 3000 m/s. The initial rod length was 0.500 m.....	22
Figure 18. Rod length for a first-order perturbation solution, a third-order perturbation solution, and the exact Tate solution. This case is for a 93% tungsten rod impacting a steel target at an impact velocity of 3000 m/s. The initial rod length was 0.500 m.....	23
Figure 19. Comparison between rod and penetration velocities for a first-order perturbation solution, a third-order perturbation solution, and the exact Tate solution. This case is for a depleted uranium rod impacting a steel target at an impact velocity of 2000 m/s. The initial rod length was 0.500 m.....	24
Figure 20. Penetration depth for a first-order perturbation solution, a third-order perturbation solution, and the exact Tate solution. This case is for a depleted uranium rod impacting a steel target at an impact velocity of 2000 m/s. The initial rod length was 0.500 m.....	25
Figure 21. Rod length for a first-order perturbation solution, a third-order perturbation solution, and the exact Tate solution. This case is for a depleted uranium rod impacting a steel target at an impact velocity of 2000 m/s. The initial rod length was 0.500 m.....	26
Figure 22. Comparison between rod and penetration velocities for a first-order perturbation solution, a third-order perturbation solution, and the exact Tate solution. This case is for a depleted uranium rod impacting a steel target at an impact velocity of 3000 m/s. The initial rod length was 0.500 m.....	27
Figure 23. Penetration depth for a first-order perturbation solution, a third-order perturbation solution, and the exact Tate solution. This case is for a depleted uranium rod impacting a steel target at an impact velocity of 3000 m/s. The initial rod length was 0.500 m.....	28
Figure 24. Rod length for a first-order perturbation solution, a third-order perturbation solution, and the exact Tate solution. This case is for a depleted uranium rod impacting a steel target at an impact velocity of 3000 m/s. The initial rod length was 0.500 m.....	29

---

## List of Tables

---

Table 1. Material input properties.....	17
Table 2. Initial values and perturbation parameters.....	23

---

## **Acknowledgments**

---

The authors would like to express their thanks to Dr. Steven Segletes of the U.S. Army Research Laboratory for his vigilance and thorough review of this report. He provided many helpful comments and suggestions during the course of the report.

INTENTIONALLY LEFT BLANK.

---

## 1. Introduction

---

The Alekseevski-Tate equations (1) have long been employed to predict the penetration of kinetic energy penetrators or rod-like projectiles. Typically, these equations are solved by straight-forward numerical integration techniques or by using the exact solution developed by Walters and Segletes (2) and refined by Segletes and Walters (3). However, due to the nonlinear nature of these equations, the exact solution yields penetration only as an implicit function of time. It is desirable to obtain an exact, albeit approximate, solution to these equations which would yield the pertinent variables, penetration velocity, penetrator length, penetrator velocity, and penetration as an explicit function of time. The analytical nature of the solutions would clearly reveal the interplay of the various terms in the governing equations on the solutions. Toward this end, as per references (1-2), a perturbation solution was obtained for the following equation set:

$$(\rho_P/2)(v-u)^2 + Y_P = (\rho_T/2)u^2 + R_T \quad (1)$$

$$\frac{dv}{dt} = \frac{-Y_P}{l\rho_P} \quad (2)$$

$$\frac{dl}{dt} = u - v \quad (3)$$

$$u = \frac{dp}{dt} \text{ or } p = \int u dt . \quad (4)$$

In these equations,  $v$  is the penetrator velocity,  $u$  is the penetration velocity,  $p$  is the penetration,  $l$  is the penetrator length,  $t$  is the time after impact,  $R_T$  is the target strength term,  $Y_P$  is the penetrator strength term,  $\rho$  represents the density, where the subscript  $P$  stands for penetrator and subscript  $T$  represents the target. First, the equations are normalized and the method of normalization will depend on the input conditions; namely, the  $\rho$  values, the initial velocity, and the strength terms. For the usual case of interest to ballisticians studying kinetic energy penetrators impacting armor targets, the following normalization parameters are introduced:

$$V = v/V_i, \quad U = u/V_i, \quad \lambda = l/L, \quad \tau = \beta t, \text{ and} \quad (5)$$

$$\mu^2 = \rho_T/\rho_P, \quad \beta = \left( \frac{\mu}{1+\mu} \right) \frac{V_i}{L}, \quad \alpha = \frac{R_T - Y_P}{Y_P}, \quad \varepsilon = \frac{Y_P}{\rho_P V_i^2}, \quad P = \frac{p}{L}, \quad (6)$$

where  $V_i$  is the impact velocity,  $L$  is the initial penetrator length, and  $V$ ,  $U$ ,  $P$ ,  $\lambda$ , and  $\tau$  are the dimensionless variables, while  $\mu$ ,  $\alpha$ ,  $\beta$ , and  $\varepsilon$  are the dimensionless constants. The parameter  $\beta$  is used to normalize the time. The constant  $\varepsilon$  is the perturbation parameter. This is the same

normalization scheme used by Forrestal et al. (4). Forrestal et al. assumed  $R_T = 0$  (i.e.,  $\alpha = -1$ ) for a steel projectile impacting a foundry core target (silica sand) at 3.0 km/s.

Thus, the normalized equations become

$$(V - U)^2 - 2\alpha\varepsilon = \mu^2 U^2, \quad (7)$$

$$\frac{dV}{d\tau} = -\frac{\varepsilon}{\lambda} \left( \frac{1+\mu}{\mu} \right), \quad (8)$$

$$\frac{d\lambda}{d\tau} = \left( \frac{1+\mu}{\mu} \right) (U - V), \quad (9)$$

and

$$P = \left( \frac{1+\mu}{\mu} \right) \int_0^\tau U d\tau. \quad (10)$$

The perturbation method, as shown by Cole (5), involves letting

$$V = V_0 + \varepsilon V_1 + \varepsilon^2 V_2 + \varepsilon^3 V_3 + \dots \quad (11)$$

$$U = U_0 + \varepsilon U_1 + \varepsilon^2 U_2 + \varepsilon^3 U_3 + \dots \quad (12)$$

$$\lambda = \lambda_0 + \varepsilon \lambda_1 + \varepsilon^2 \lambda_2 + \varepsilon^3 \lambda_3 + \dots \quad (13)$$

$$P = P_0 + \varepsilon P_1 + \varepsilon^2 P_2 + \varepsilon^3 P_3 + \dots \quad (14)$$

and the perturbation parameter  $\varepsilon = \frac{Y_P}{\rho_P V_i^2} \ll 1$  is chosen.

For example, if a third-order perturbation solution is obtained, terms of the order of  $\varepsilon$  to the fourth power are neglected. Hence, the accuracy of the solution depends on the magnitude of  $\varepsilon$  and the number of terms in the above equation set.

One can substitute the expressions for  $V$ ,  $U$ ,  $\lambda$ , and  $P$  (equations 11–14) into the nondimensional equation set (equations 7–10) and obtain, to order zero (considering only terms involving  $\varepsilon^0$ ), the following set:

$$(V_0 - U_0)^2 = \mu^2 U_0^2, \quad (15)$$

$$\frac{dV_0}{d\tau} = 0, \quad (16)$$

and

$$\frac{d\lambda_0}{d\tau} = -\left( \frac{1+\mu}{\mu} \right) (V_0 - U_0), \quad (17)$$

where the initial conditions at  $\tau = 0$  are  $V_0(0) = 1$ ,  $\lambda_0(0) = 1$ .

The solution is

$$V_0 = 1 , \quad (18)$$

$$U_0 = \frac{1}{1 + \mu} , \quad (19)$$

$$\lambda_0 = 1 - \tau , \quad (20)$$

and

$$P_0 = \frac{\tau}{\mu} , \quad (21)$$

in agreement with Forrestal et al. (4).

Proceeding along these same lines (next consider terms of order  $\varepsilon$ , etc.), one can calculate  $V_0$ ,  $V_1$ ,  $V_2$ ,  $V_3$ , and the corresponding  $U$ ,  $P$ , and  $\lambda$  values. The method is straight forward but tedious. The final equations, to the third order, are

$$V = V_0 + \varepsilon V_1 + \varepsilon^2 V_2 + \varepsilon^3 V_3 , \quad (22)$$

$$U = U_0 + \varepsilon U_1 + \varepsilon^2 U_2 + \varepsilon^3 U_3 , \quad (23)$$

$$\lambda = \lambda_0 + \varepsilon \lambda_1 + \varepsilon^2 \lambda_2 + \varepsilon^3 \lambda_3 , \quad (24)$$

and

$$P = P_0 + \varepsilon P_1 + \varepsilon^2 P_2 + \varepsilon^3 P_3 , \quad (25)$$

where

$$V_1 = \Theta \ln \Pi ,$$

$$V_2 = \Theta^2 \Omega \left[ \ln \Pi + \frac{1}{\Pi} - 1 \right] - \frac{1}{2} \Theta^2 [\ln \Pi]^2 ,$$

$$V_3 = \Theta^3 \left[ \Psi \ln \Pi - \frac{\Omega^2}{2\Pi^2} + \left( 2\Omega + 2\Omega^2 - \frac{\alpha^2}{2\mu} + \frac{\alpha^2}{2\mu^2} \right) \frac{1}{\Pi} - 2\Omega (\ln \Pi)^2 + \frac{1}{2} (\ln \Pi)^3 - \Omega \frac{\ln \Pi}{\Pi} + C_3 \right] ,$$

$$U_1 = \left( \frac{1}{\mu} \right) [\ln \Pi - \alpha] ,$$

$$U_2 = \frac{V_2}{1 + \mu} + \frac{\alpha}{\mu^2} (1 + \mu) \ln \Pi + \frac{\alpha^2}{2\mu^3} (1 - \mu^2) ,$$

$$U_3 = \frac{V_3}{1 + \mu} - \frac{\alpha \Theta^2}{\mu} \left[ \frac{3(\ln \Pi)^2}{2} + \left( \frac{3}{2} - \frac{5\Omega}{2} - \frac{3\alpha}{2} \right) \ln \Pi - \frac{\Omega}{\Pi} + \left( \frac{1}{2} \left( \frac{\alpha}{\mu} (1 - \mu) \right)^2 + \Omega \right) \right] ,$$

$$\lambda_1 = \Theta [\tau \Omega + \Pi \ln \Pi] ,$$

$$\lambda_2 = \Theta^2 \left[ - \left( 3 - \frac{3\alpha}{\mu} - \frac{\alpha^2}{2\mu} + \frac{\alpha^2}{2\mu^2} \right) \Pi + \Omega \ln \Pi + 2\Omega \Pi \ln \Pi - \frac{1}{2} \Pi (\ln \Pi)^2 + C_{\lambda_2} \right],$$

$$\lambda_3 = \Theta^3 \left[ - \frac{7\Omega}{2} \Pi (\ln \Pi)^2 + \Sigma \ln \Pi + \Phi \Pi \ln \Pi + \Gamma \Pi - \frac{\Omega}{2} (\ln \Pi)^2 + \frac{\Omega^2}{2\Pi} + \frac{\Pi (\ln \Pi)^3}{2} \right] + C_{\lambda_3},$$

$$P_1 = - \frac{\Theta}{\mu} [\tau(1+\alpha) + \Pi \ln \Pi],$$

$$P_2 = \frac{\Theta^2}{\mu} \left[ \left( 3 + \alpha + \frac{\alpha^2}{2} - \frac{2\alpha}{\mu} - \frac{\alpha^2}{2\mu} \right) \Pi - \Omega \ln \Pi - \left( 2 + \alpha - \frac{\alpha}{\mu} \right) \Pi \ln \Pi + \frac{1}{2} \Pi (\ln \Pi)^2 \right] + C_{P_2},$$

$$P_3 = - \frac{\Theta^3}{\mu} \left[ \left( \xi - \frac{\Omega^2}{2} \right) \Pi + \omega \Pi \ln \Pi + \frac{\Omega^2}{2\Pi} + \vartheta \ln \Pi + \delta \Pi (\ln \Pi)^2 - \frac{\Omega}{2} (\ln \Pi)^2 + \frac{1}{2} \Pi (\ln \Pi)^3 \right] + C_{P_3},$$

and

$$\Psi = \left( 4 - \frac{5\alpha}{\mu} - \frac{\alpha^2}{2\mu} + \frac{3\alpha^2}{2\mu^2} \right),$$

$$\Pi = 1 - \tau,$$

$$\Theta = \frac{(1+\mu)}{\mu},$$

$$\Omega = 1 - \frac{\alpha}{\mu},$$

$$C_3 = - \frac{3\Omega^2}{2} - 2\Omega - \frac{1}{2} \left( \frac{\alpha}{\mu} \right)^2 (1-\mu),$$

$$\Sigma = \frac{7\Omega^2}{2} - \frac{\alpha^2}{2\mu} + \frac{1}{2},$$

$$\Phi = 2 + 5\Omega + 4\Omega^2 - \frac{2\alpha^2}{\mu},$$

$$\Gamma = - \frac{5}{2} - 7\Omega^2 - 5\Omega + \frac{5\alpha^2}{2\mu} + \frac{\alpha^3}{2\mu^3} (\mu-1)^2,$$

$$\xi = -4 - 3\Omega^2 - 7\Omega + \frac{9\alpha^2}{2\mu} - 5\alpha - \frac{3\alpha^2}{2} - \frac{\alpha^3}{2\mu^2} (1-\mu)^2,$$

$$\omega = \frac{7}{2} + 6\Omega + 3\alpha\Omega + \frac{3\Omega^2}{2} + \alpha + \frac{3\alpha^2}{2},$$

$$\begin{aligned} \vartheta &= \Omega + \frac{5\Omega^2}{2} + \alpha - \frac{3\alpha^2}{2\mu} + \frac{1}{2}, \\ \delta &= -2\Omega - \frac{3}{2}(1+\alpha), \\ C_{\lambda_2} &= 3 - \frac{3\alpha}{\mu} - \frac{\alpha^2}{2\mu} + \frac{\alpha^2}{2\mu^2}, \\ C_{\lambda_3} &= \Theta^3 \left( \frac{5}{2} + \frac{13\Omega^2}{2} + 5\Omega - \frac{5\alpha^2}{2\mu} - \frac{\alpha^3}{2\mu^3} (\mu-1)^2 \right), \\ C_{P2} &= -\frac{\Theta^2}{\mu} \left( 3 + \alpha + \frac{\alpha^2}{2} - \frac{2\alpha}{\mu} - \frac{\alpha^2}{2\mu} \right), \end{aligned}$$

and

$$C_{P3} = \frac{\Theta^3 \xi}{\mu}.$$

The normalization scheme used is deemed appropriate for ballistic applications, namely tungsten rods penetrating steel. The third-order solution for  $U$ ,  $V$ ,  $P$ , and  $\lambda$ , with comparison to the exact Alekseevski-Tate equation solution, is shown in figures 1–3. In this case,  $V_i = 2$  km/s,  $L = 0.5$  m,  $\rho_p = 17,600$  kg/m<sup>3</sup>,  $Y_p = 1.0$  GPa,  $\rho_T = 7,800$  kg/m<sup>3</sup>, and  $R_T = 5.5$  GPa. The perturbation parameter computes as  $\varepsilon = 0.0142$ , which is much less than one and terms with a coefficient of  $\varepsilon^4$  were neglected. The agreement is excellent up to about 495  $\mu$ s for the velocities and nearly identical for the rod length and penetration. The exact (Tate) solution terminates at about 518  $\mu$ s. The appendix lists the FORTRAN program used to calculate the rod velocity, penetration velocity, rod length, and penetration all as a function of time.

A few comments are in order. All equations contain a term like  $\ln(1-\tau)$ . Thus, a singularity occurs at  $\tau = 1$  or  $t = \frac{L(1+\mu)}{\mu V_i} = 625.5$   $\mu$ s for the case described. Thus,  $t$  must be less than this

value for the perturbation solution to be evaluated. As this singularity is approached, deviation from the exact solution occurs. Hence, one can accurately calculate the perforation of finite thickness targets if the penetration time is less than this value. As an example, figures 4–6 plot the rod velocity, penetration velocity, penetration, and rod length for a tungsten rod impacting a finite-thickness (25 mm) steel plate as described, except the initial rod length was 39.12 mm. The first-order and third-order perturbation theories are compared with the Tate solution. Again, the agreement is excellent. Note that the first-order perturbation theory also agrees very well with the exact solution for this case. Thus, approximate formulae may be derived for the perforation of thin plates. The first order equations are

$$V = 1 + \varepsilon \Theta \ln \Pi, \quad (26)$$

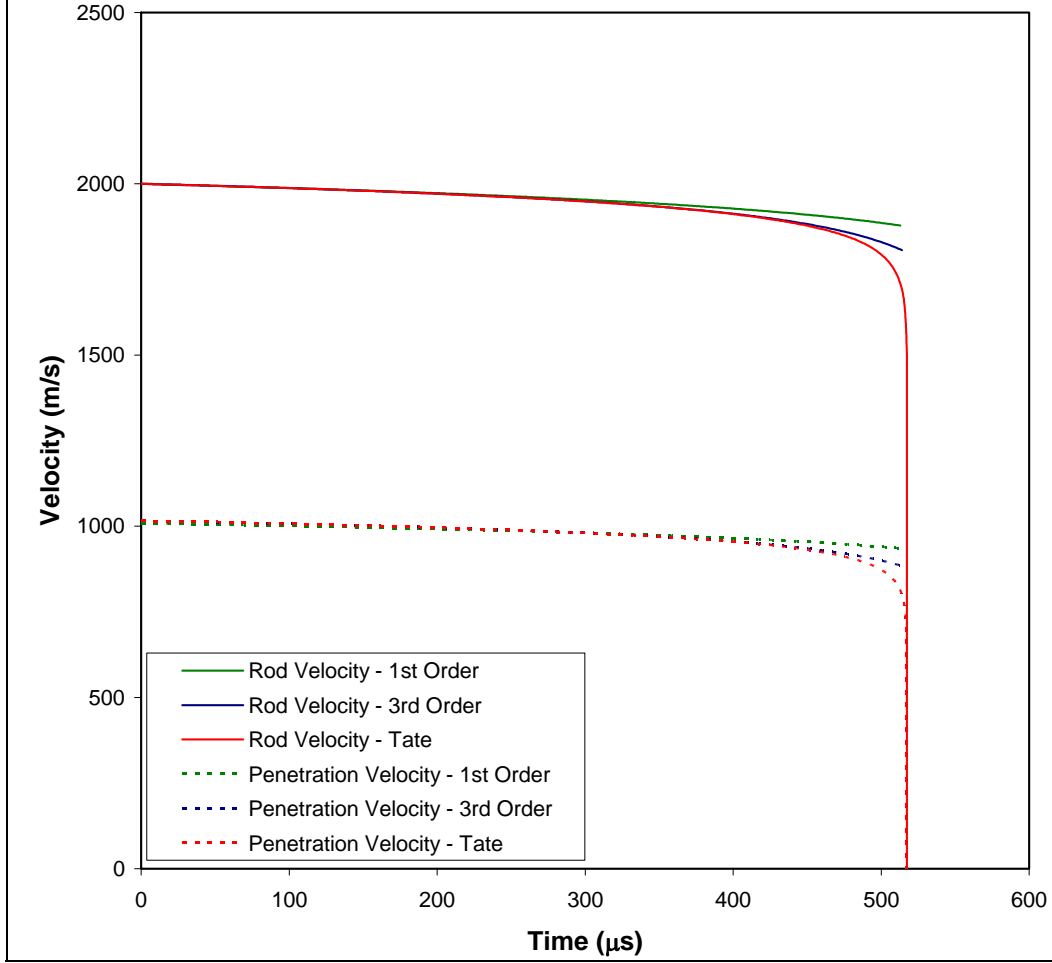


Figure 1. Comparison between rod and penetration velocities for a first-order perturbation solution, a third-order perturbation solution, and the exact Tate solution. This case is for a tungsten rod impacting a steel target at an impact velocity of 2000 m/s. The initial rod length was 0.500 m.

$$U = \frac{1}{1+\mu} + \frac{\varepsilon}{\mu} [\ln \Pi - \alpha] , \quad (27)$$

$$\lambda = \Pi + \varepsilon \Theta [\Omega(1-\Pi) + \Pi \ln \Pi] , \quad (28)$$

and

$$P = \frac{1-\Pi}{\mu} - \frac{\varepsilon \Theta}{\mu} [(1-\Pi)(\alpha+1) + \Pi \ln \Pi] . \quad (29)$$

When  $P=H$ , the finite target plate thickness, equation 29 can be solved for the event duration in terms of  $\Pi$  as

$$\Pi = \exp \left[ \frac{-1}{A\Pi} \left( \frac{H}{L} + \frac{\Pi-1}{\mu} \right) - \frac{(1-\Pi)}{\Pi} (\alpha+1) \right] \text{ and } A = \frac{\varepsilon \Theta}{\mu} . \quad (30)$$

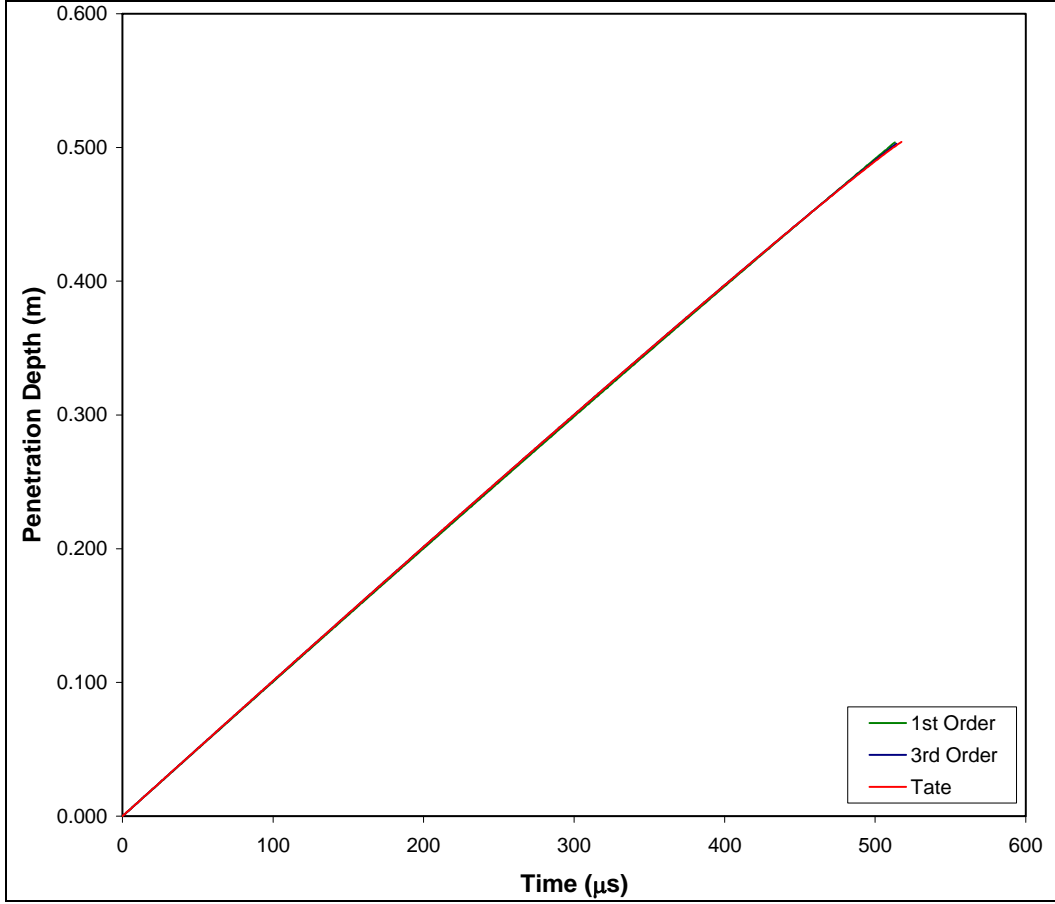


Figure 2. Penetration depth for a first-order perturbation solution, a third-order perturbation solution, and the exact Tate solution. This case is for a tungsten rod impacting a steel target at an impact velocity of 2000 m/s. The initial rod length was 0.500 m.

Further, the exponential term in equation 30 may be approximated by the first two terms of its series expansion or  $\exp[x] = 1 + x$ . In this case,

$$\Pi = \frac{B + \sqrt{B^2 + 4C}}{2} \text{ where } B = 2 + \alpha - \frac{1}{A\mu} \text{ and } C = -\frac{H}{AL} + \frac{1}{A\mu} - (\alpha + 1) . \quad (31)$$

From equation 31, the time,  $t$ , was 25.34  $\mu\text{s}$  and the time calculated from the more exact equation 30 via standard iteration techniques was 25.12  $\mu\text{s}$ . The rod velocity was 1948.156 m/s according to the approximate theory and 1943.000 m/s from the Tate solution. The penetration velocity was 977.524 m/s vs. 976.500 m/s from the Tate solution. The final rod length was 14.20 mm vs. 14.70 mm from the Tate solution. This close agreement means that the perturbation solution is in excellent agreement with the Tate solution for small times, even for a first-order perturbation solution. Forrestal et al. (4) also showed good agreement with Tate for short times.

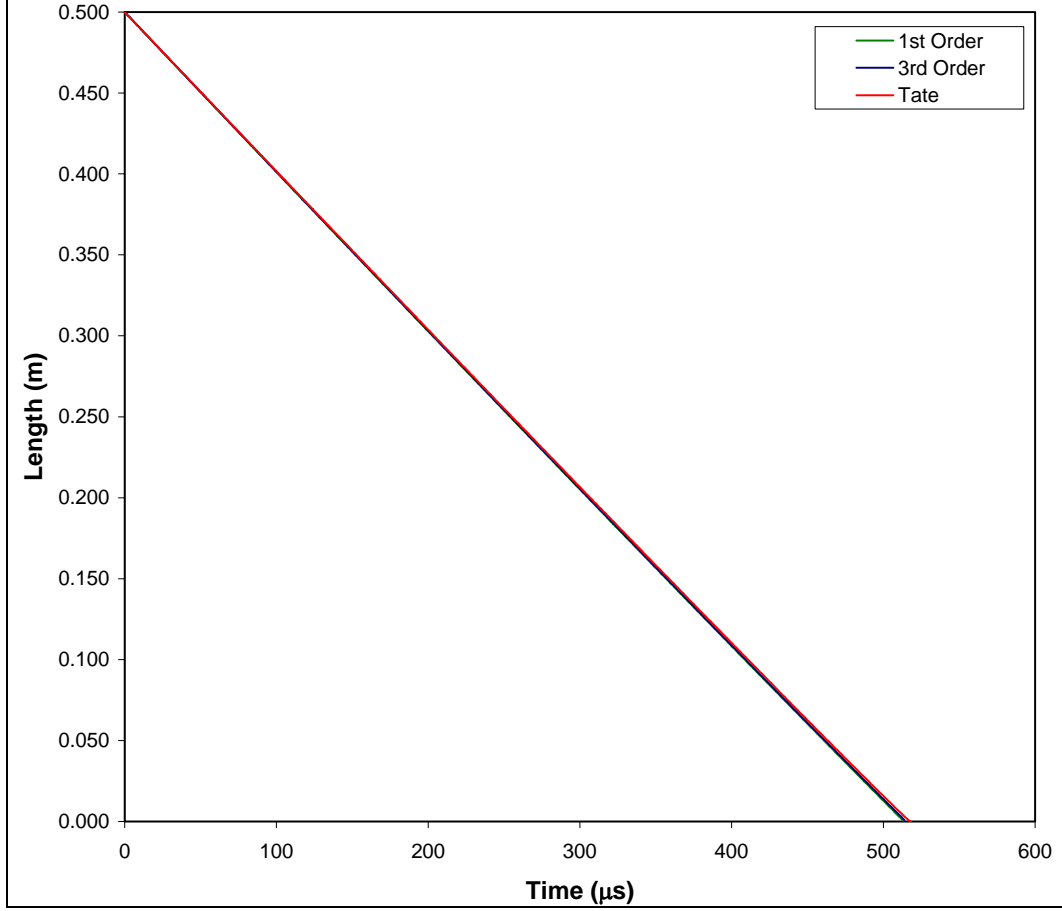


Figure 3. Rod length for a first-order perturbation solution, a third-order perturbation solution, and the exact Tate solution. This case is for a tungsten rod impacting a steel target at an impact velocity of 2000 m/s. The initial rod length was 0.500 m.

As previously mentioned, the perturbation parameter must be much less than one. The value of  $\varepsilon$  used in the above equations implies a small penetrator strength or  $Y_p \ll \rho_p V_i^2$ . If this is not the case, for example, for a soft target, i.e., small  $R_T$ , the equations can be normalized with

$$V = v/V_i, \quad U = u/V_i, \quad \lambda = l/L, \quad P = \frac{p}{L}, \quad (32)$$

$$\mu^2 = \rho_T / \rho_P, \quad \beta = \left( \frac{\mu}{1 + \mu} \right) \frac{V_i}{L}, \quad \alpha = \frac{Y_p - R_T}{R_T}, \quad \varepsilon = \frac{R_T}{\rho_P V_i^2}, \quad \tau = \beta t, \quad (33)$$

and the equation set becomes

$$(V - U)^2 + 2\alpha\varepsilon = \mu^2 U^2, \quad (34)$$

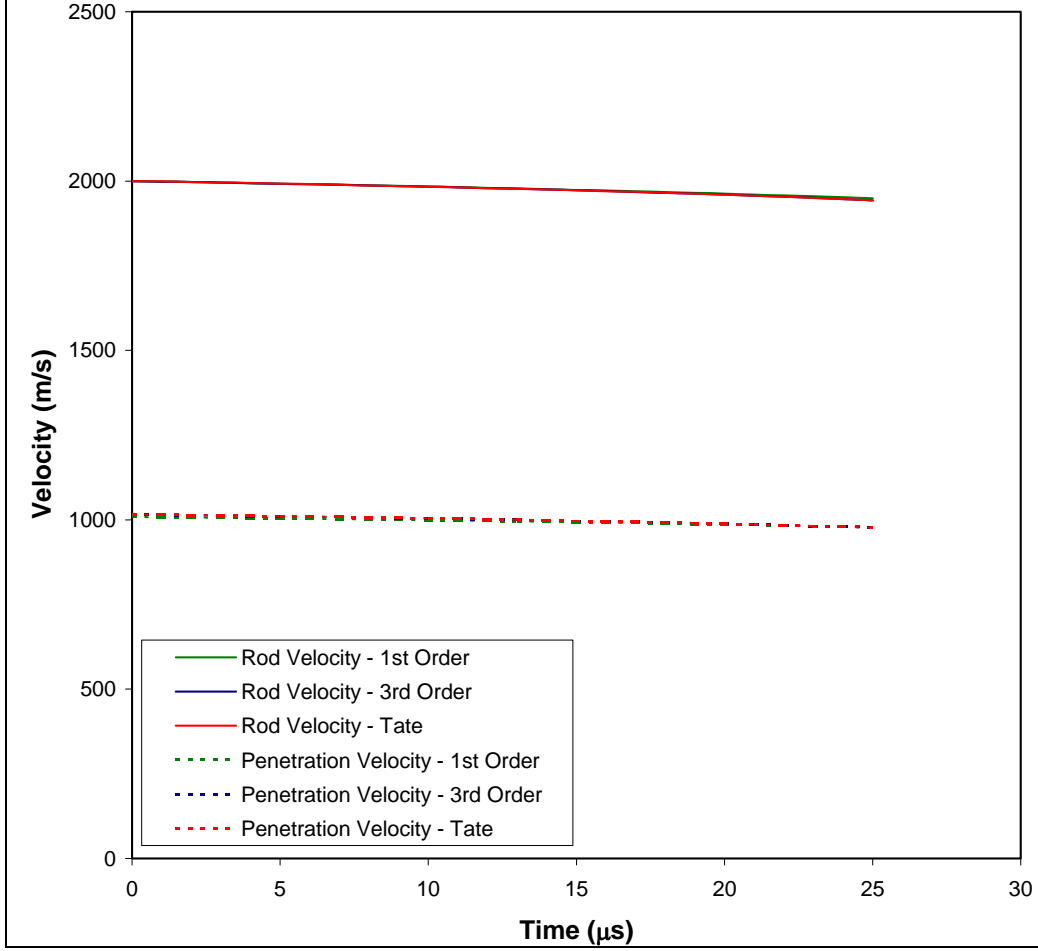


Figure 4. Comparison between rod and penetration velocities for a first-order perturbation solution, a third-order perturbation solution, and the exact Tate solution. This case is for a tungsten rod impacting a 25-mm-thick steel target at an impact velocity of 2000 m/s. The initial rod length was 0.03912 m.

$$\frac{dV}{d\tau} = -\frac{\varepsilon}{\lambda} \left( \frac{1+\mu}{\mu} \right) \left( \frac{Y_p}{R_T} \right), \quad (35)$$

and

$$\frac{d\lambda}{d\tau} = \left( \frac{1+\mu}{\mu} \right) (U - V). \quad (36)$$

This is very similar to the previous set of equations and thus follows the same solution scheme.

Note that the normalization scheme was initiated by dividing the first equation by  $\rho_p$  and defining  $\mu^2$  to be  $\rho_T/\rho_p$ . Alternately, one could divide the equation by  $\rho_T$  and define  $\mu^2$  to be  $\rho_p/\rho_T$ .

Other normalization schemes are possible namely if the nondimensional variables are defined as

$$\lambda = l/L, \quad \mu = \rho_T/\rho_p, \quad K = \frac{Y_p}{\rho_p}, \quad \Sigma = \frac{2(R_T - Y_p)}{\rho_p}, \quad (37)$$

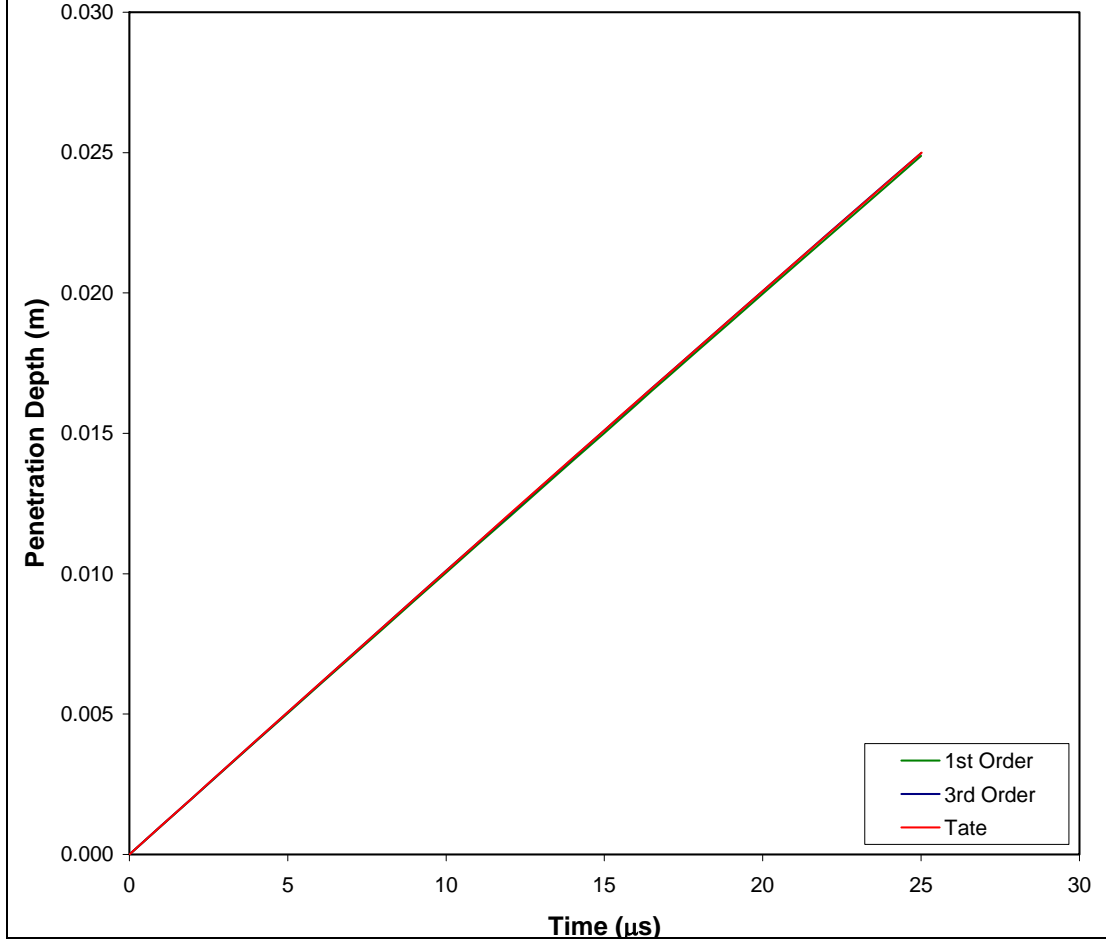


Figure 5. Penetration depth for a first-order perturbation solution, a third-order perturbation solution, and the exact Tate solution. This case is for a tungsten rod impacting a 25-mm-thick steel target at an impact velocity of 2000 m/s. The initial rod length was 0.03912 m.

$$V = v/\sqrt{\Sigma}, \quad U = u/\sqrt{\Sigma}, \quad \lambda = l/\sqrt{\Sigma}, \quad \tau = t\sqrt{\Sigma}/L, \quad P = p/L. \quad (38)$$

Note that  $\Sigma > 0$  is required. Based on input, if this is not the case, one may reformulate  $\Sigma$  as  $\frac{2(Y_p - R_T)}{\rho_T}$ .

The equation set becomes

$$(U - V)^2 = \mu U^2 + 1, \quad (39)$$

$$\frac{d\lambda}{d\tau} = U - V, \quad \text{and} \quad (40)$$

$$\frac{\lambda dV}{d\tau} = \frac{-K}{\Sigma} = \frac{-Y_p}{2(R_T - Y_p)} \quad \text{or} \quad \frac{dV}{d\tau} = \frac{\varepsilon}{\lambda}, \quad (41)$$

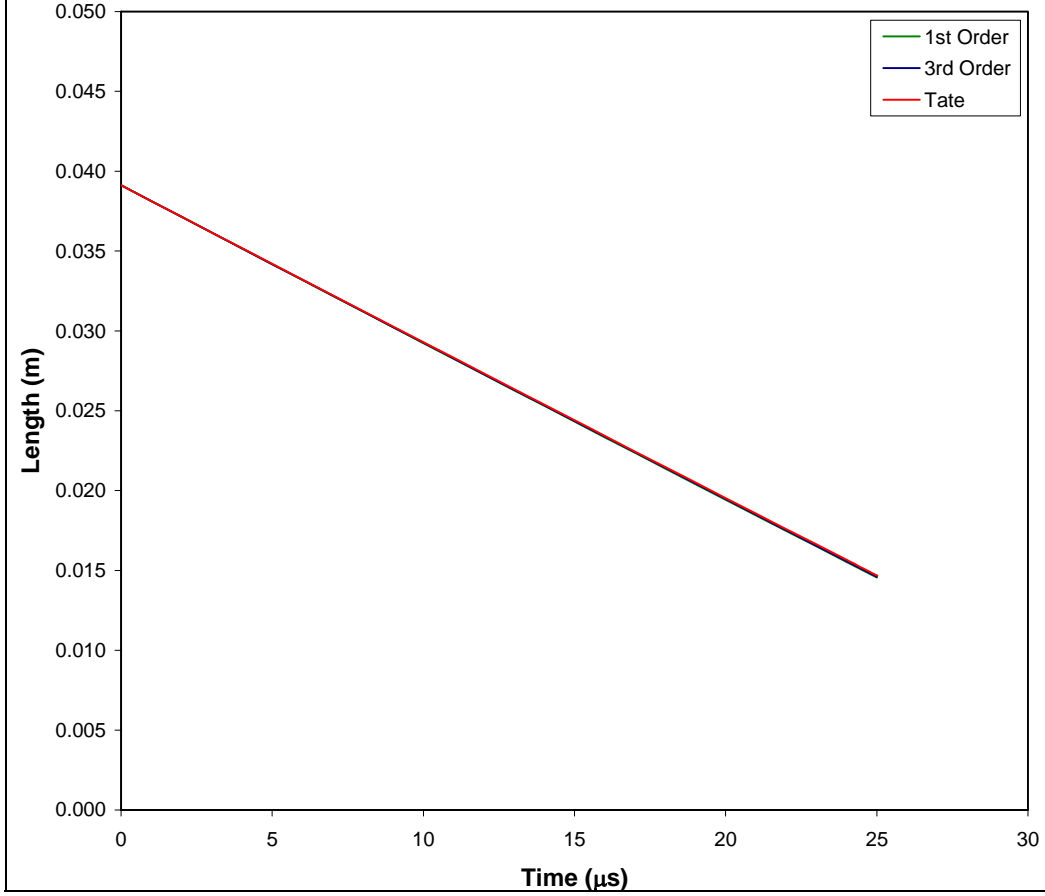


Figure 6. Rod length for a first-order perturbation solution, a third-order perturbation solution, and the exact Tate solution. This case is for a tungsten rod impacting a 25-mm-thick steel target at an impact velocity of 2000 m/s. The initial rod length was 0.03912 m.

where  $\varepsilon = \frac{-K}{\Sigma} = \frac{-Y_p}{2(R_T - Y_p)}$  is chosen to be the perturbation parameter. Again, the previous set of equations is very similar to the original set of equations and thus follows the same solution scheme. The normalization scheme or equation set chosen will depend on the input conditions (known initial values) and the requirement to keep  $\varepsilon \ll 1$ . Also, it is advantageous to make the time where the logarithmic singularity occurs ( $\tau = 1$ ) as large as possible.

---

## 2. Parametric Studies

---

Other rod-target configurations were studied using the third-order perturbation theory in order to exercise the model. In figure 7, the rod velocity and penetration velocity are plotted vs. time for the Tate solution, the first-order, and the third-order perturbation theory. In this case, the initial rod velocity was 3 km/s. The agreement between the third-order perturbation model and the

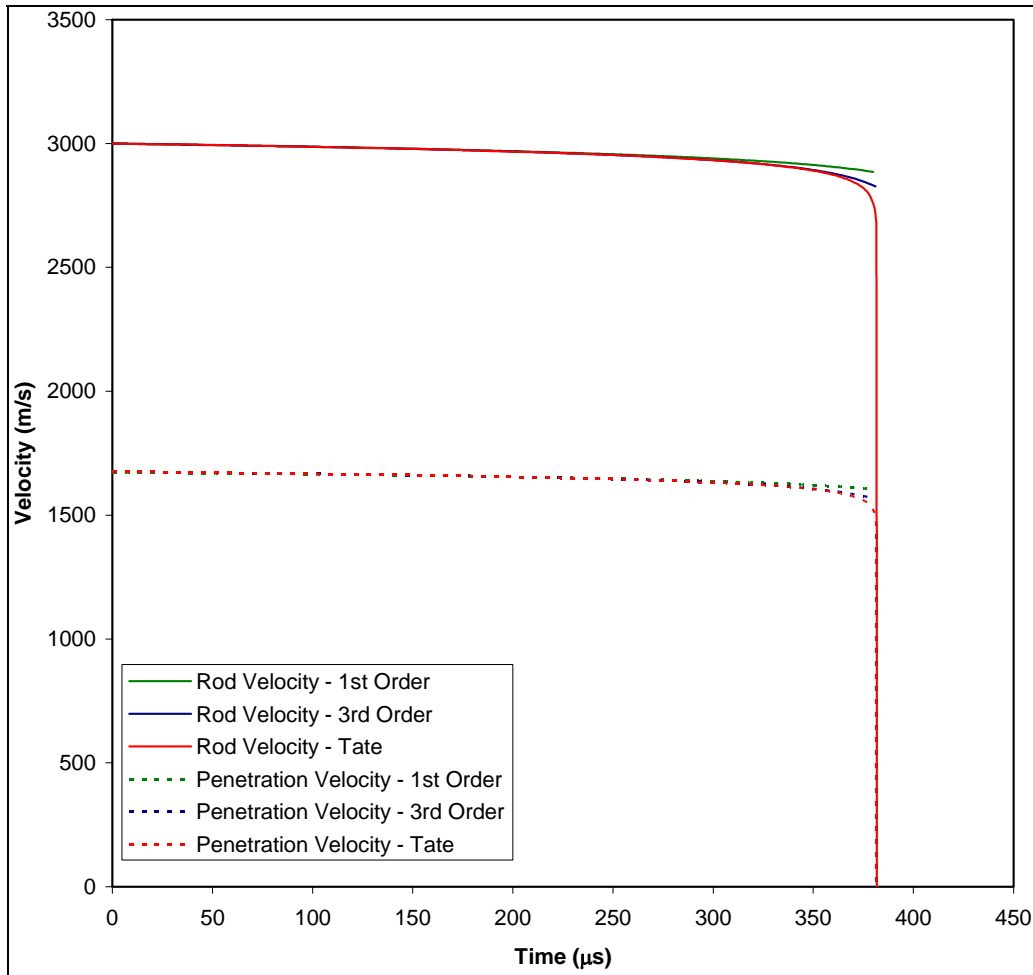


Figure 7. Comparison between rod and penetration velocities for a first-order perturbation solution, a third-order perturbation solution, and the exact Tate solution. This case is for a tungsten rod impacting a steel target at an impact velocity of 3000 m/s. The initial rod length was 0.500 m.

Tate solution is excellent, due to the perturbation parameter  $\epsilon = 0.0063$ , being small. The length and penetration are also in excellent agreement, as shown in figures 8 and 9. The input, namely the strength terms, was obtained from Dr. Steven Segletes of ARL for the tungsten rod vs. the RHA target.

Next, figures 10–12 plot the velocities, penetration, and rod length vs. time for the case studied by Forrestal et al. (4), namely a steel rod impacting a geological (silica-sand) target. The first-order solution, third-order solution, and the Tate solution are compared. The perturbation parameter was 0.0192 and the improvement of the third-order solution over the first-order solution is shown. The Tate solution completes the penetration process at 56  $\mu\text{s}$ . The first-order solution agrees, within 1%, up to 29  $\mu\text{s}$ , which is the Forrestal et al. (4) solution. The third-order solution is valid, again within 1%, to 35  $\mu\text{s}$ .

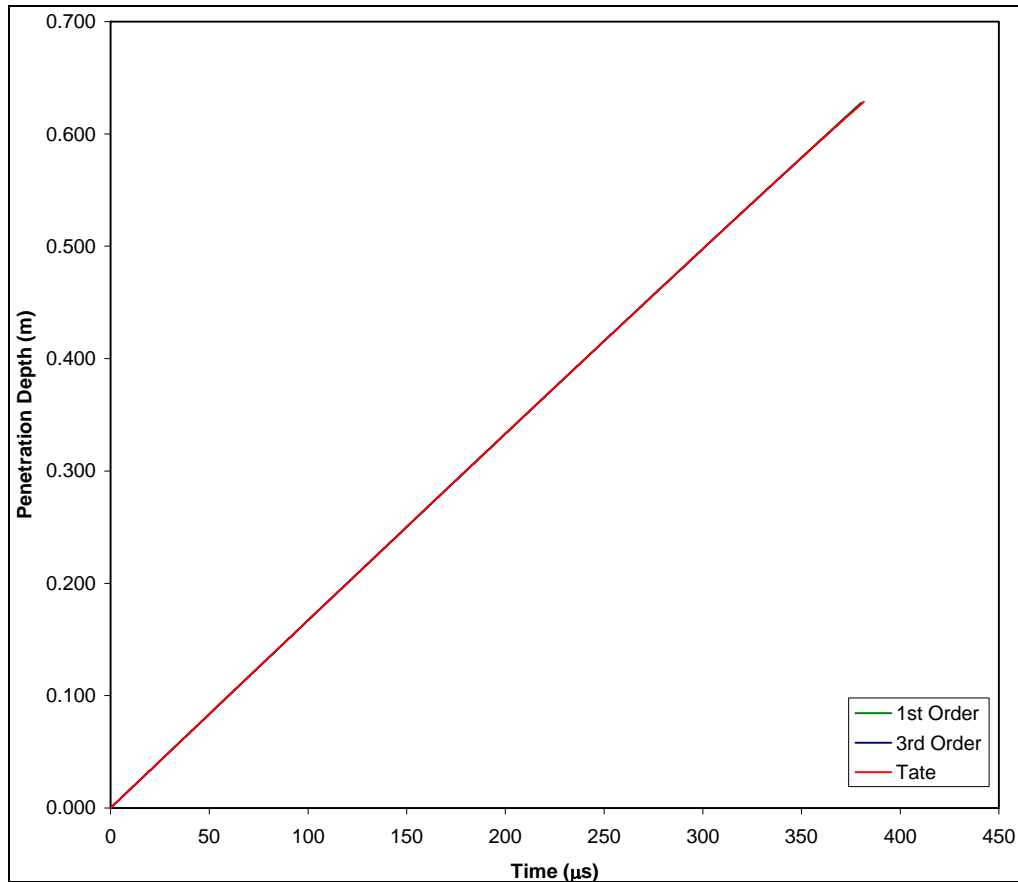


Figure 8. Penetration depth for a first-order perturbation solution, a third-order perturbation solution, and the exact Tate solution. This case is for a tungsten rod impacting a steel target at an impact velocity of 3000 m/s. The initial rod length was 0.500 m.

As mentioned previously, the strength terms for the steel targets were obtained from Dr. Segletes. Input values used by Edward Horwath of ARL were penetrator strengths of 3.6 GPa for tungsten, 3.2 GPa for depleted uranium (DU), and the target resistance was 5.1 GPa for RHA. All input values used in this study are recorded in table 1. These tungsten values, and the value previously given for the RHA target, are designated as 93% tungsten (the only difference in the two tungstens is the value assigned to  $Y_p$ ) and the plots are shown in figures 13–15 for an initial rod velocity of 2 km/s. Again, the agreement is good. The Tate solution indicates that the penetration process is complete at 652  $\mu$ s and the third-order solution is valid up to 598  $\mu$ s. Figures 16–18 present the same plots for an initial impact velocity of 3 km/s. In this case, again because of the lower value of the perturbation parameter, the agreement is excellent. The Tate solution terminates at 428  $\mu$ s and the third-order theory is valid up to 409  $\mu$ s. The perturbation parameter was 0.0511 for the 2 km/s case and 0.0227 for the 3 km/s case. Table 2 lists the perturbation parameters for all cases. Finally, figures 19–21 give the plots for an initial velocity of 2 km/s for a DU rod impacting RHA. The agreement is good, with the Tate solution terminating at 640.5  $\mu$ s and the third-order solution valid up to 611  $\mu$ s. The agreement is perfect for the same rod/target configuration at an initial impact velocity of 3 km/s, see figures 22–24.

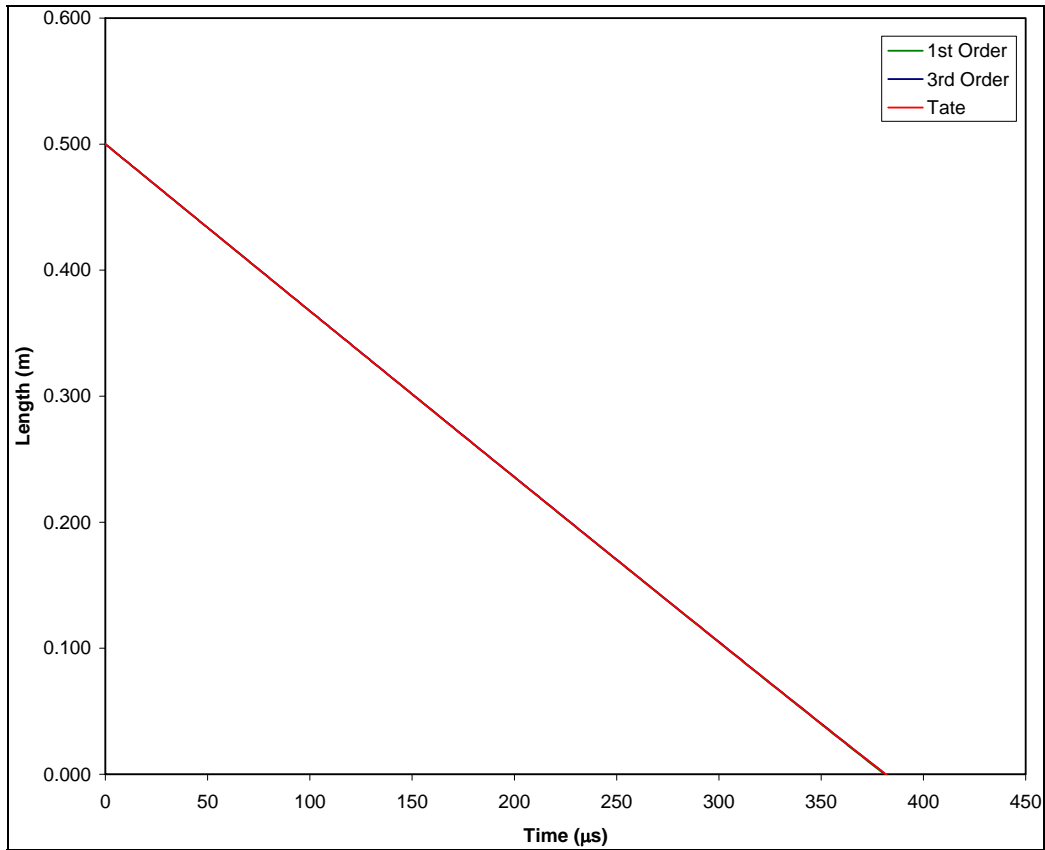


Figure 9. Rod length for a first-order perturbation solution, a third-order perturbation solution, and the exact Tate solution. This case is for a tungsten rod impacting a steel target at an impact velocity of 3000 m/s. The initial rod length was 0.500 m.

Here, the perturbation parameter was 0.0430 for the 2 km/s case and 0.0191 for the 3 km/s case. All input and perturbation values are summarized in tables 1 and 2.

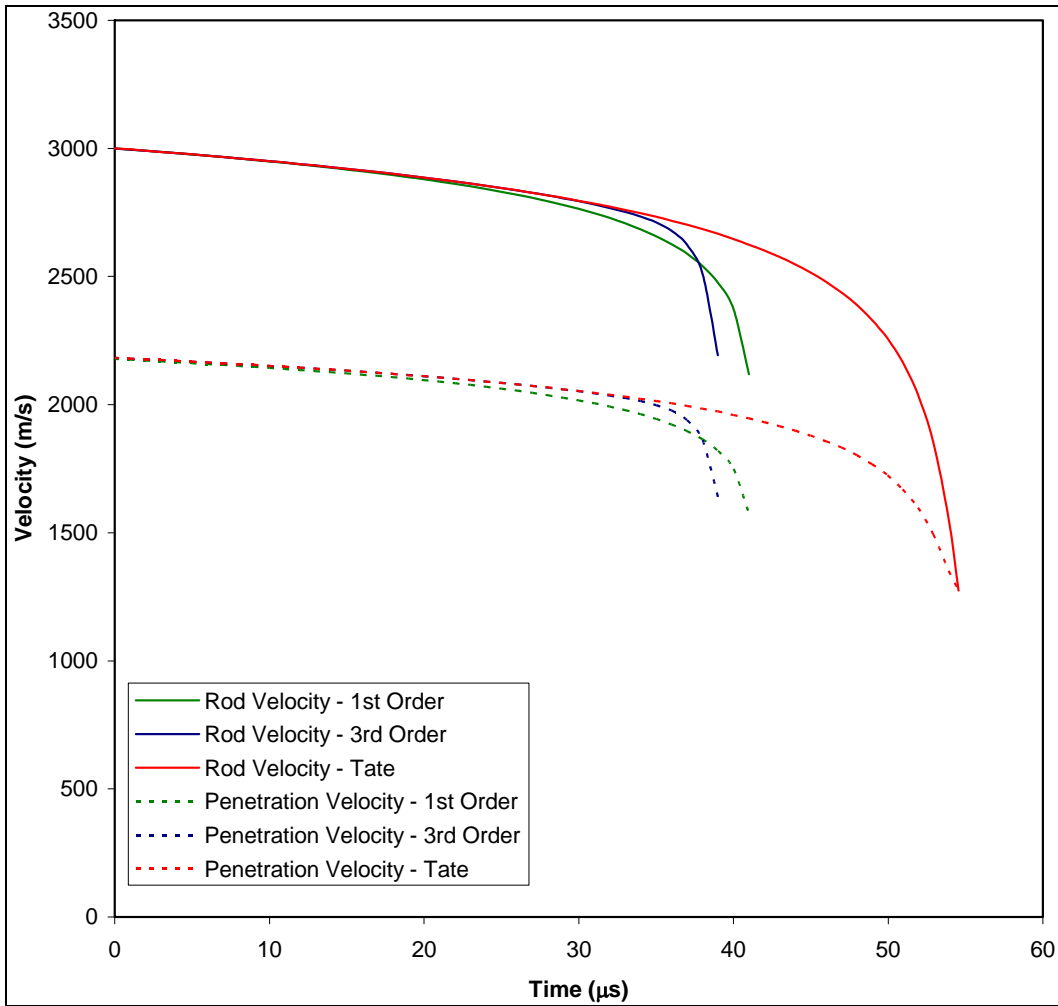


Figure 10. Comparison between rod and penetration velocities for a first-order perturbation solution, a third-order perturbation solution, and the exact Tate solution. This case is for a steel rod impacting a silica-sand target at an impact velocity of 3000 m/s. The initial rod length was 0.03912 m.

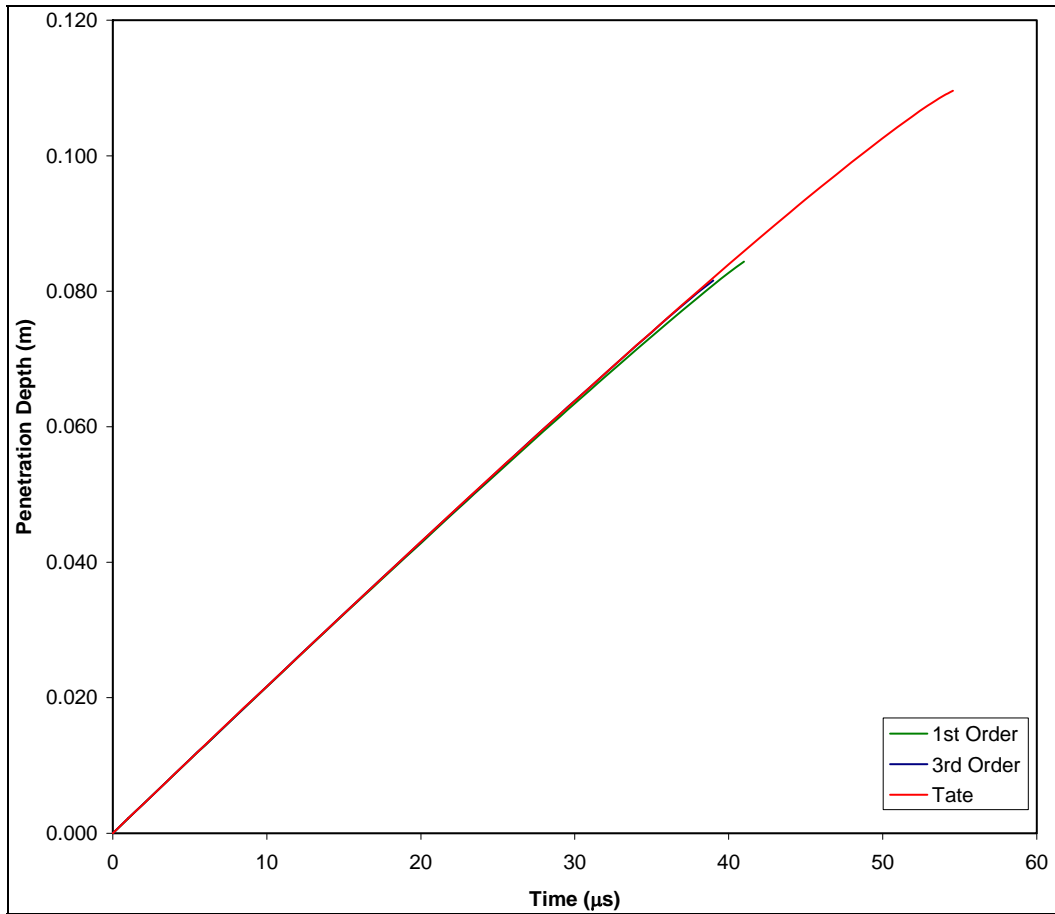


Figure 11. Penetration depth for a first-order perturbation solution, a third-order perturbation solution, and the exact Tate solution. This case is for a steel rod impacting a silica-sand target at an impact velocity of 3000 m/s. The initial rod length was 0.03912 m.

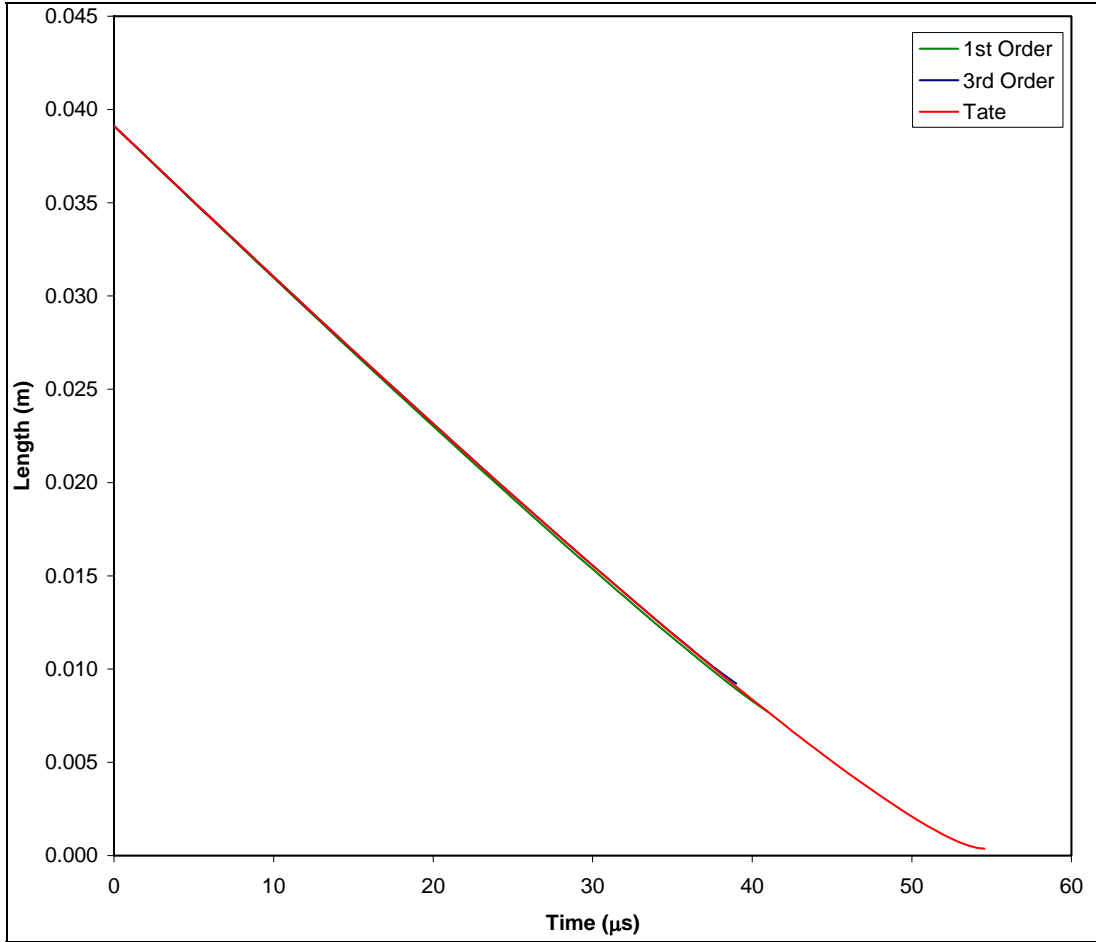


Figure 12. Rod length for a first-order perturbation solution, a third-order perturbation solution, and the exact Tate solution. This case is for a steel rod impacting a silica-sand target at an impact velocity of 3000 m/s. The initial rod length was 0.03912 m.

Table 1. Material input properties.

<b>Material</b>	<b><math>\rho_P</math> (kg/m<sup>3</sup>)</b>	<b><math>\rho_T</math> (kg/m<sup>3</sup>)</b>	<b><math>Y_P</math> (GPa)</b>	<b><math>R_T</math> (GPa)</b>
Tungsten	17600	—	1.000	—
93% tungsten	17600	—	3.600	—
Depleted uranium (DU)	18600	—	3.200	—
Steel (RHA)	—	7800	—	5.500
Steel (RHA) for 93% tungsten	—	7800	—	5.100
Forrestal penetrator (steel)	8000	—	1.380	—
Forrestal target (silica-sand)	—	1700	—	0.000

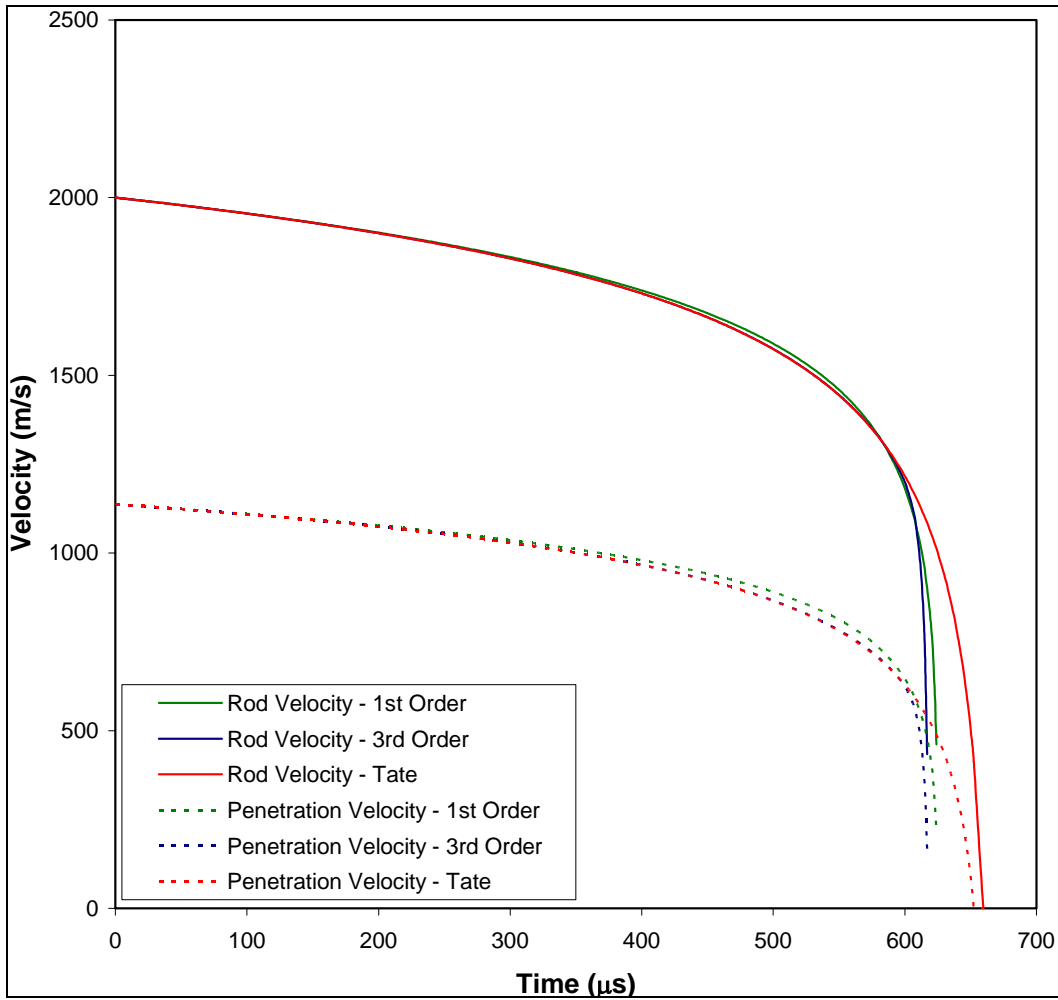


Figure 13. Comparison between rod and penetration velocities for a first-order perturbation solution, a third-order perturbation solution, and the exact Tate solution. This case is for a 93% tungsten rod impacting a steel target at an impact velocity of 2000 m/s. The initial rod length was 0.500 m.

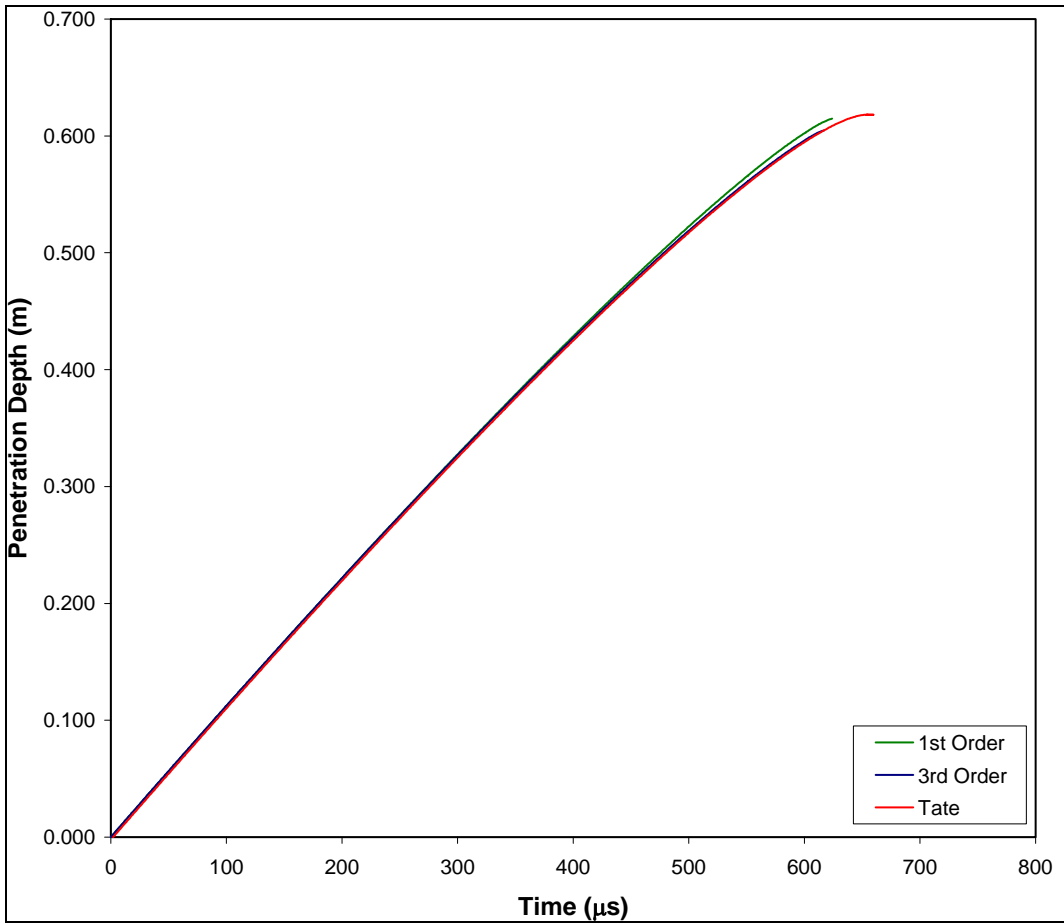


Figure 14. Penetration depth for a first-order perturbation solution, a third-order perturbation solution, and the exact Tate solution. This case is for a 93% tungsten rod impacting a steel target at an impact velocity of 2000 m/s. The initial rod length was 0.500 m.

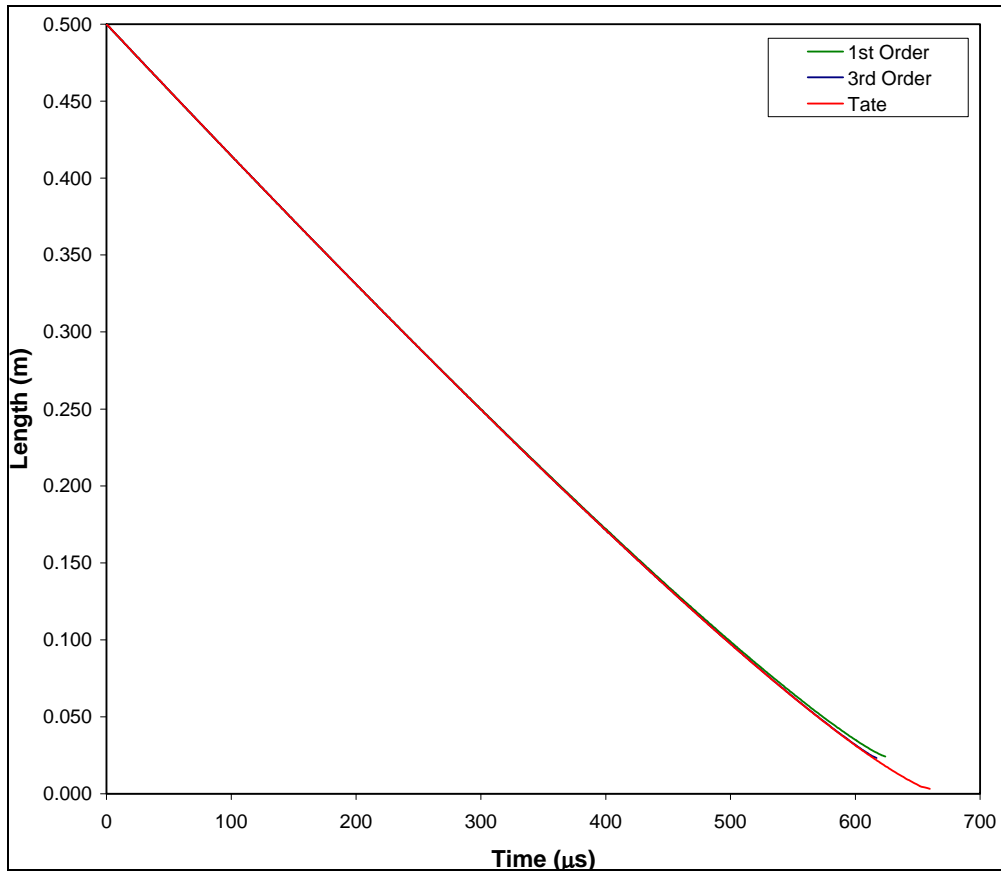


Figure 15. Rod length for a first-order perturbation solution, a third-order perturbation solution, and the exact Tate solution. This case is for a 93% tungsten rod impacting a steel target at an impact velocity of 2000 m/s. The initial rod length was 0.500 m.

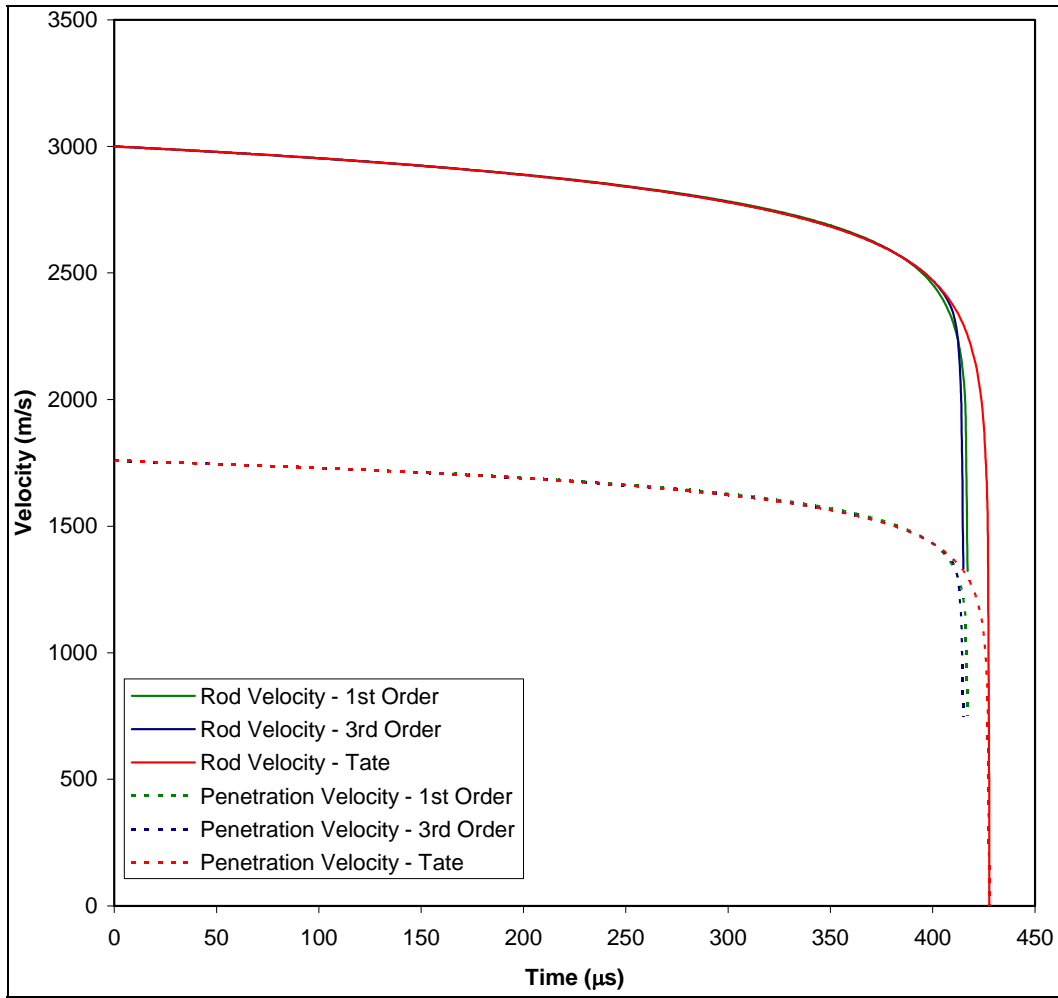


Figure 16. Comparison between rod and penetration velocities for a first-order perturbation solution, a third-order perturbation solution, and the exact Tate solution. This case is for a 93% tungsten rod impacting a steel target at an impact velocity of 3000 m/s. The initial rod length was 0.500 m.

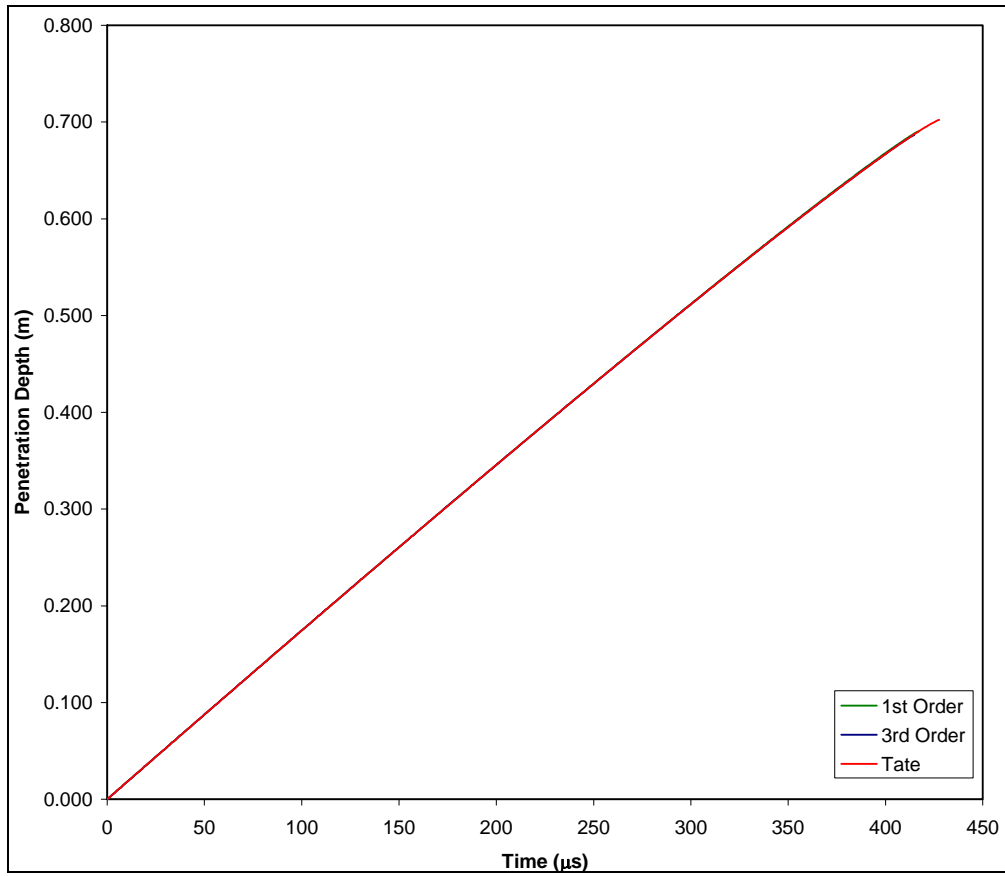


Figure 17. Penetration depth for a first-order perturbation solution, a third-order perturbation solution, and the exact Tate solution. This case is for a 93% tungsten rod impacting a steel target at an impact velocity of 3000 m/s. The initial rod length was 0.500 m.

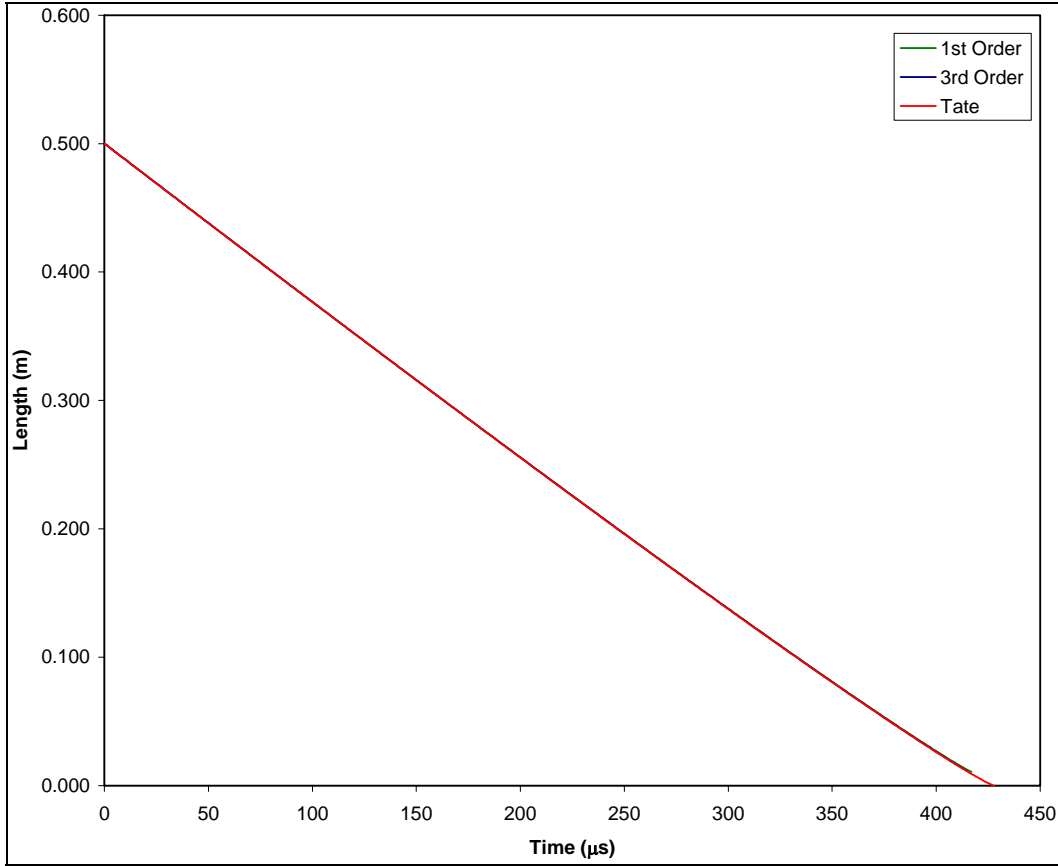


Figure 18. Rod length for a first-order perturbation solution, a third-order perturbation solution, and the exact Tate solution. This case is for a 93% tungsten rod impacting a steel target at an impact velocity of 3000 m/s. The initial rod length was 0.500 m.

Table 2. Initial values and perturbation parameters.

Penetrator	Target	$L_o$ (m)	$V_i$ (m/s)	$\epsilon$
Tungsten	Steel (RHA)	0.500	2000	0.0140
Tungsten	Steel (RHA)	0.500	3000	0.0063
93% tungsten	Steel (RHA)	0.500	2000	0.0511
93% tungsten	Steel (RHA)	0.500	3000	0.0227
Depleted uranium (DU)	Steel (RHA)	0.500	2000	0.0430
Depleted uranium (DU)	Steel (RHA)	0.500	3000	0.0191
Forrestal steel	Silica-sand	0.039	3000	0.0192

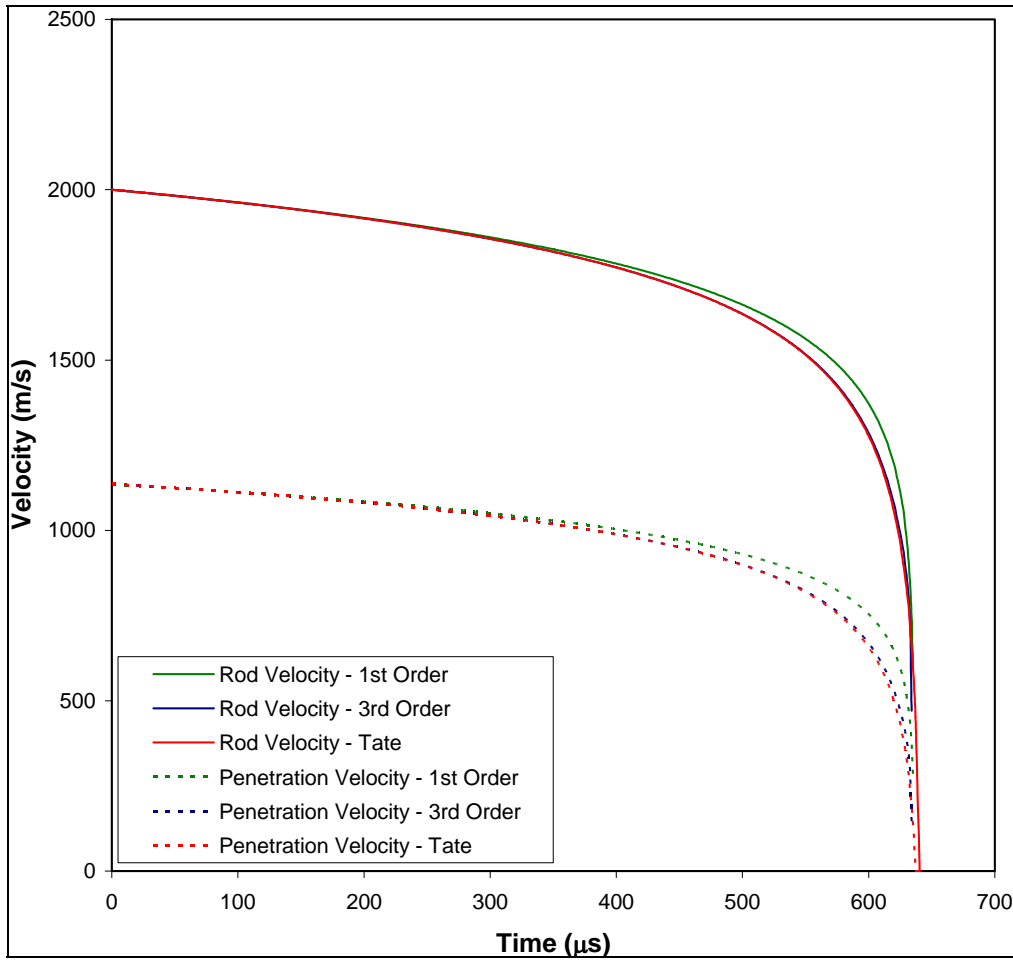


Figure 19. Comparison between rod and penetration velocities for a first-order perturbation solution, a third-order perturbation solution, and the exact Tate solution. This case is for a depleted uranium rod impacting a steel target at an impact velocity of 2000 m/s. The initial rod length was 0.500 m.

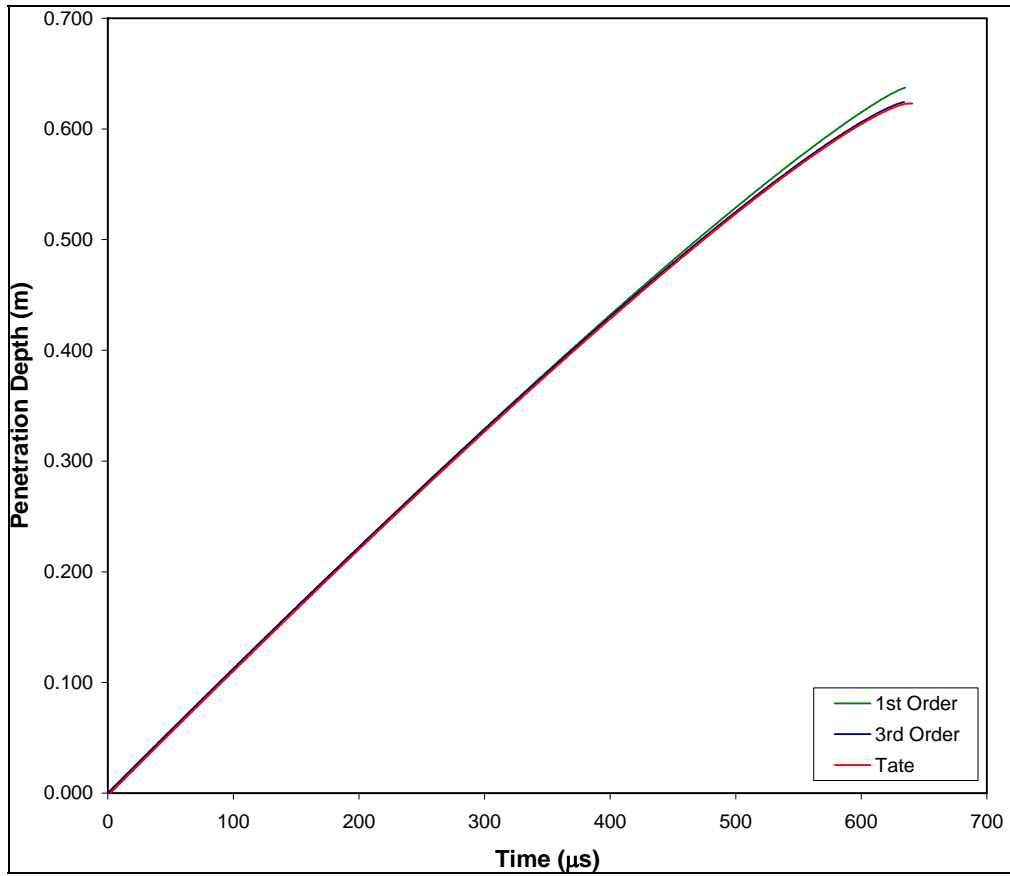


Figure 20. Penetration depth for a first-order perturbation solution, a third-order perturbation solution, and the exact Tate solution. This case is for a depleted uranium rod impacting a steel target at an impact velocity of 2000 m/s. The initial rod length was 0.500 m.

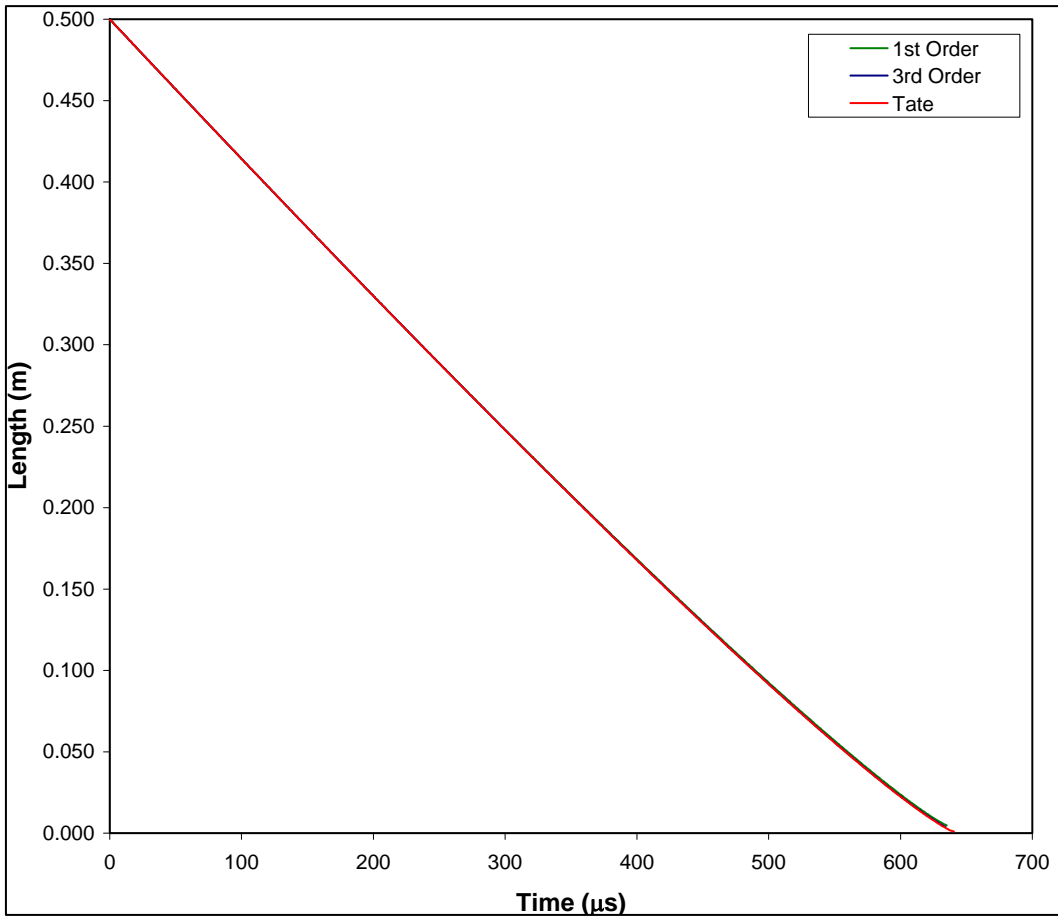


Figure 21. Rod length for a first-order perturbation solution, a third-order perturbation solution, and the exact Tate solution. This case is for a depleted uranium rod impacting a steel target at an impact velocity of 2000 m/s. The initial rod length was 0.500 m.

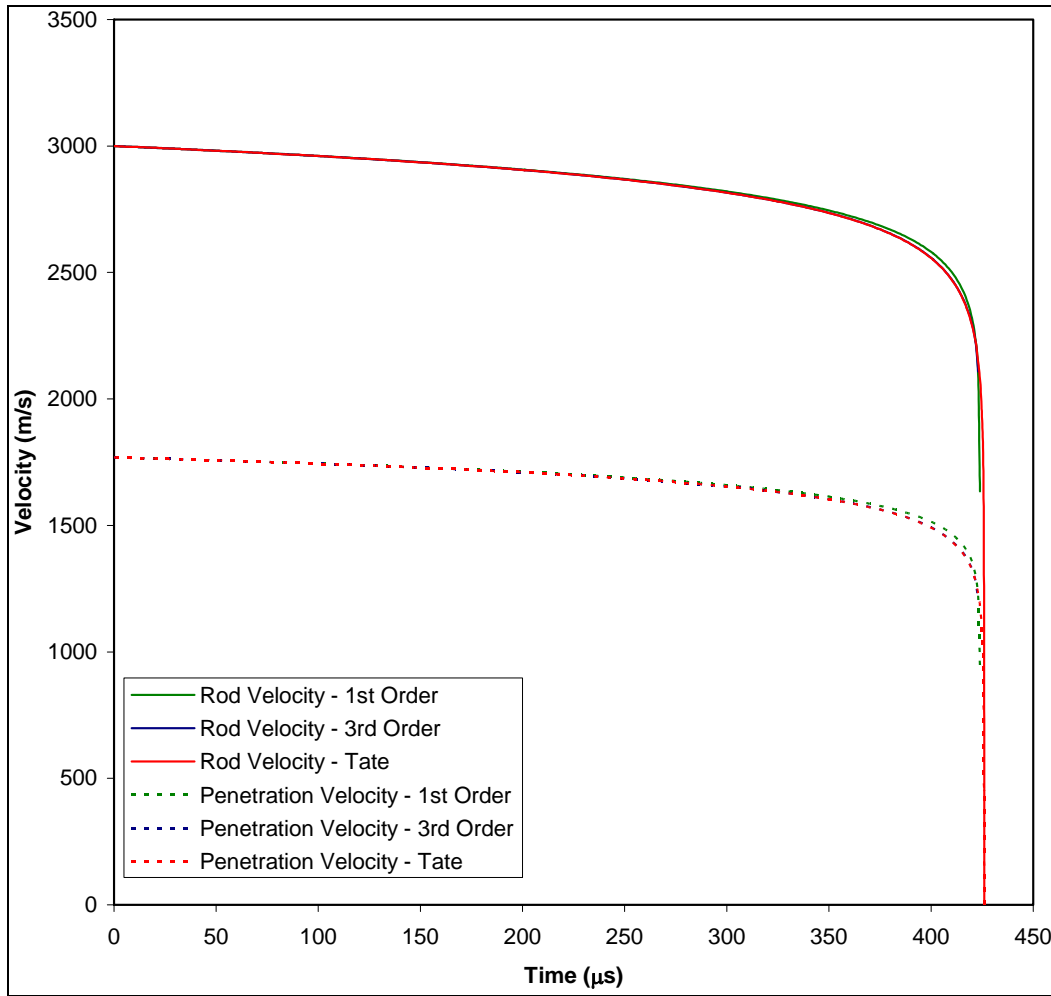


Figure 22. Comparison between rod and penetration velocities for a first-order perturbation solution, a third-order perturbation solution, and the exact Tate solution. This case is for a depleted uranium rod impacting a steel target at an impact velocity of 3000 m/s. The initial rod length was 0.500 m.

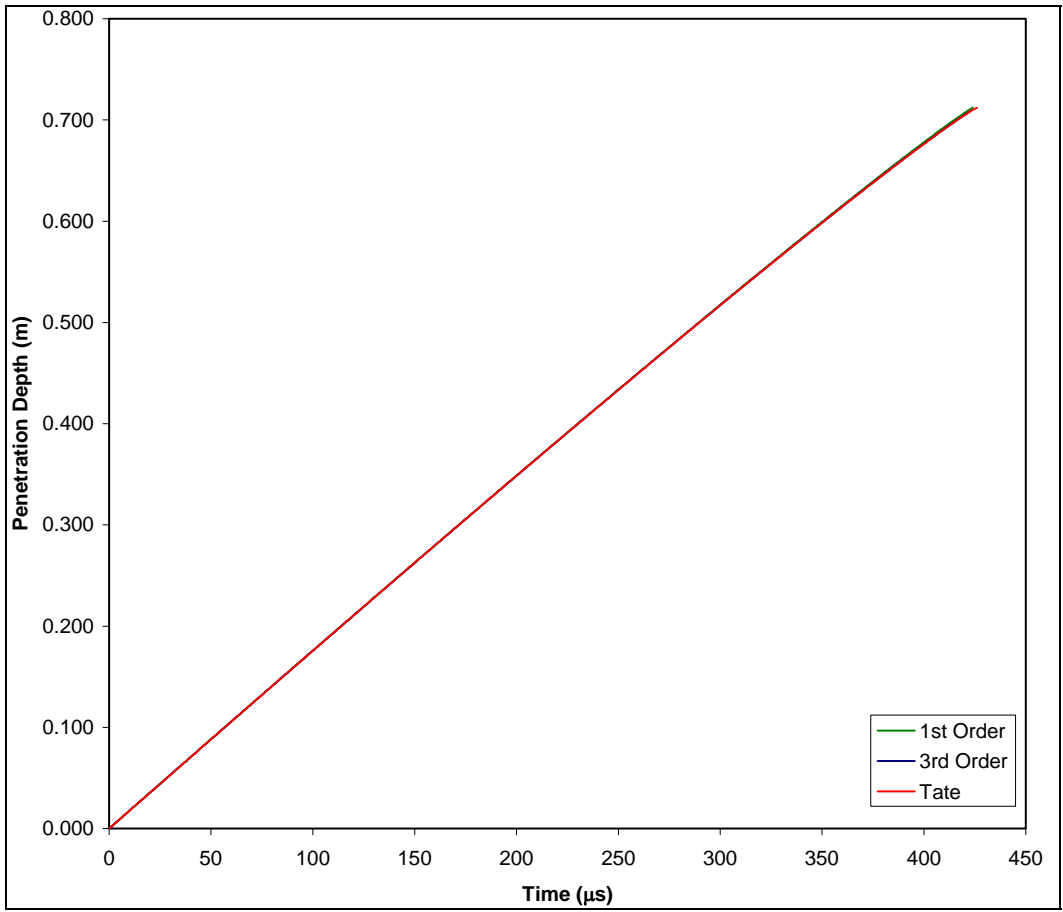


Figure 23. Penetration depth for a first-order perturbation solution, a third-order perturbation solution, and the exact Tate solution. This case is for a depleted uranium rod impacting a steel target at an impact velocity of 3000 m/s. The initial rod length was 0.500 m.

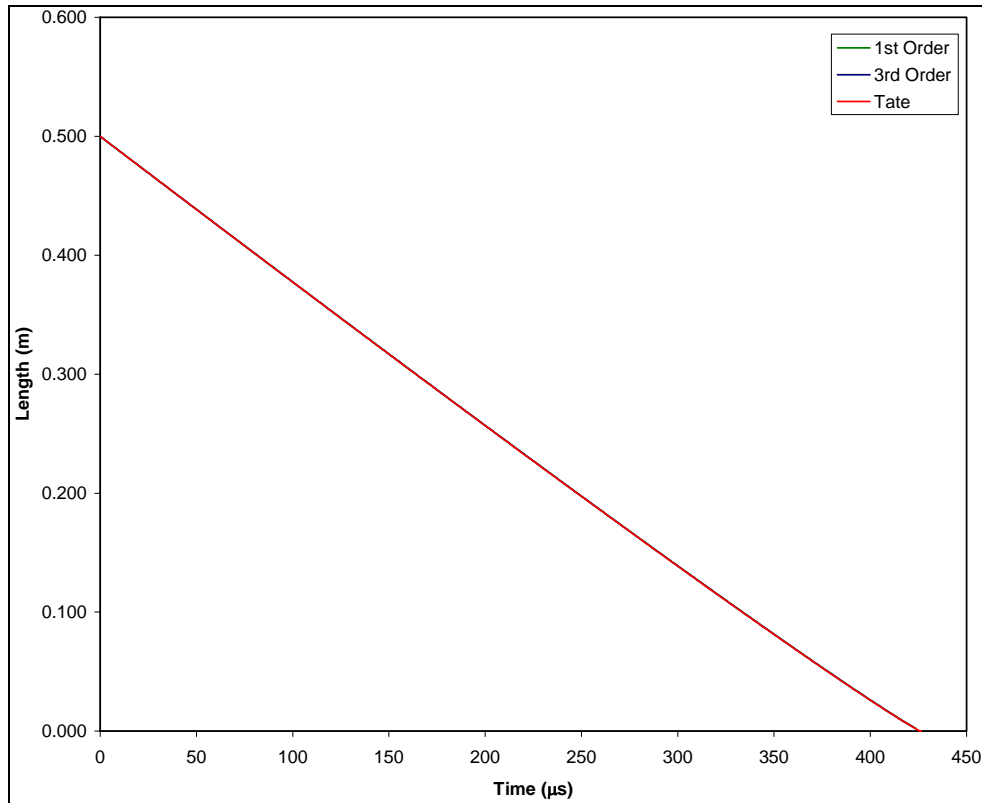


Figure 24. Rod length for a first-order perturbation solution, a third-order perturbation solution, and the exact Tate solution. This case is for a depleted uranium rod impacting a steel target at an impact velocity of 3000 m/s. The initial rod length was 0.500 m.

---

### 3. Conclusions

---

A perturbation solution of the Alekseevski-Tate equations was obtained through the third order. Agreement with the exact solution is excellent for a tungsten rod impacting a steel target at a velocity of 2.0 km/s, as well as for other cases of interest to ballisticians involved in the penetration of steel targets. Also, the velocities and residual length of a tungsten rod perforating a finite-thickness steel plate show excellent agreement with the exact equations. The approximate (perturbation) solution yields the dependent variables ( $V$ ,  $U$ ,  $\lambda$ , and  $P$ ) as explicit functions of time. Also, alternate forms of the normalization of the pertinent equations are investigated to obtain a perturbation parameter much less than one for various penetration problems depending on the input conditions, namely target and penetrator densities, strengths, and initial impact conditions. Also, comments are made regarding the singularity in time. Extensions of the method to higher orders (i.e., the fourth order) are possible, but a point of diminishing returns has been reached. The current third-order solution is expressible as an algebraic equation, amenable to a spread sheet or simple calculator evaluation.

---

## 4. References

---

1. Tate, A. A Theory for the Deceleration of Long Rods after Impact. *J. Mech. Phys. Solids* **1967**, *15*, 387–399.
2. Walters, W. P.; Segletes, S. B. An Exact Solution of the Long Rod Penetration Equations. *International Journal of Impact Engineering* **1991**, *11* (2), 225–231.
3. Segletes, S. B.; Walters, W. P. Extensions to the Exact Solution of the Long-Rod Penetration/Erosion Equations. *International Journal of Impact Engineering* **2003**, *11*, 363–376.
4. Forrestal, M. J.; Piekutowski, A. J.; Luk, V. K. Long-Rod Penetration into Simulated Geological Targets at an Impact Velocity of 3.0 km/s. Presented at the *11th International Symposium on Ballistics*, Brussels, Belgium, 9–11 May 1989, Vol. 2.
5. Cole, J. D. *Perturbation Methods in Applied Mathematics*. Blaisdell Publishing Company: Waltham, MA, 1968.

---

## Appendix. FORTRAN Computer Program

---

```

! Pertubation.f90
!
! FUNCTIONS:
! Pertubation - Closed-form equations for Tate's model from a pertubation analysis.
!
!*****!
! PROGRAM: Pertubation
!
! PURPOSE: This program calculates the rod velocity, penetration velocity, penetration
!          depth, and instantaneous length using pertubation method up to the third-order
!          correction terms.
!*****!

      program Pertubation

      implicit none

      ! Identifiers
      ! RT: Strength resistance of target (Kg/m.s^2)
      ! RHO_P: Density of penetrator (Kg/m^3)
      ! RHO_T: Density of target (Kg/m^3)
      ! YP: Flow stress of penetrator (Pa)
      ! VI: Impact velocity (m/s)
      ! VR: Rod velocity (m/s)
      ! UP: Penetration velocity (m/s)
      ! LO: Original length of penetrator (m)
      ! LI: Instantaneous length of rod (m)
      ! P: Penetration Depth (m)
      ! T: Time (microsecond)
      ! VN: Normalized rod velocity
      ! UN: Normalized penetration velocity
      ! PD: Normalized penetration depth
      ! LAMDA: Normalized length
      ! TAU: Normalized time
      ! MHU: Dimensionless variable
      ! BETA: Dimensionless variable
      ! ALPHA: Dimensionless variable
      ! EPSI: Dimensionless variable
      ! A,B: Expressions used for equation compactness

      DOUBLEPRECISION RT, RHO_P, RHO_T, YP, VI, VR, UP, LO, LI, P, PD, T, VN, UN, LAMDA, TAU,
      MHU, BETA, ALPHA, EPSI, V0, U0, LAMDA0, PD0, V1, U1, LAMDA1, PD1, V2, U2, LAMDA2, PD2, V, U,
      C0, C1, C2, C3, V3, U3, PD3, LAMDA3, THK, A, B

      INTEGER:: ORDER

      ! Input values for velocity, length, and material constants

```

```

PRINT*, "Enter impact velocity of penetrator, 'Meters per Second'"
READ*, VI

PRINT*, "Enter original length of penetrator, 'Meters'"
READ*, LO

PRINT*, "Enter density of penetrator material, 'Kilograms per Meter Cubed'"
READ*, RHO_P

PRINT*, "Enter density of target material, 'Kilograms per Meter Cubed'"
READ*, RHO_T

PRINT*, "Enter flow stress of penetrator material, 'Pascals'"
READ*, YP

PRINT*, "Strength resistance of target, 'Pascals'"
READ*, RT

!      Check for data inconsistencies
!      The "strength resistance of the target (RT)," cannot be equal to the "flow stress of the
!      penetrator (YP)," for the perturbation solution to be meaningful.

IF(RT.EQ.YP)THEN

PRINT*, "*****RT must not equal YP for a meaningful perturbation solution.*****"

STOP

ENDIF

PRINT*, "Thickness of the target, 'Meters'"

READ*, THK

!      Assume a semi-infinite plate for zero thickness.

IF(THK.EQ.0)THEN
    THK=1
ENDIF

PRINT*, "What order perturbation solution do you require"

READ*, ORDER

OPEN(UNIT=12, FILE="Perturbation.dat", STATUS="OLD")

!      Normalization scheme

MHU=SQRT(RHO_T/RHO_P)

BETA=MHU/(1.0+MHU)*VI/LO

ALPHA=(RT-YP)/YP

EPSI=YP/(RHO_P*VI**2)

```

$$A=(1.0+MHU)/MHU$$

$$B=1.0-ALPHA/MHU$$

$$T=0.0$$

DO

$$TAU=BETA*T$$

! Zero order calculation resulting from pertubation analysis

$$V0=1.0$$

$$U0=1.0/(1.0+MHU)$$

$$LAMDA0=1.0-TAU$$

$$PD0=TAU/MHU$$

! First order calculation resulting from pertubation analysis

$$V1=((1.0+MHU)/MHU)*LOG(1.0-TAU)$$

$$U1=(1.0/MHU)*(LOG(1.0-TAU)-ALPHA)$$

$$LAMDA1=((1.0+MHU)/MHU)*((1.0-ALPHA/MHU)*TAU+(1.0-TAU)*LOG(1.0-TAU))$$

$$PD1=-((1.0+MHU)/(MHU**2))*(TAU*(ALPHA+1.0)+(1.0-TAU)*LOG(1.0-TAU))$$

! Second order calculation resulting from pertubation analysis

$$V2=((1.0+MHU)/MHU)**2*(1.0-ALPHA/MHU)*(LOG(1.0-TAU)+1/(1.0-TAU)-1.0)- & 0.5*((1.0+MHU)/MHU)**2*(LOG(1.0-TAU))**2$$

$$U2=V2/(1.0+MHU)+(ALPHA/MHU**2)*(1.0+MHU)*LOG(1.0-TAU)+(ALPHA**2)*(1.0- & MHU**2)/(2.0*MHU**3)$$

$$C0=3.0-3.0*ALPHA/MHU+ALPHA**2/(2.0*MHU**2)-ALPHA**2/(2.0*MHU)$$

$$LAMDA2=((1.0+MHU)/MHU)**2*(-(3.0-3.0*ALPHA/MHU+ALPHA**2/(2.0*MHU**2))- & ALPHA**2/(2.0*MHU))*(1-TAU)+(1.0-ALPHA/MHU)*LOG(1.0-TAU)+2.0*(1.0- & ALPHA/MHU)*(1.0-TAU)*LOG(1.0-TAU)-0.5*(1.0-TAU)* (LOG(1.0-TAU))**2+C0$$

$$PD2=(1.0+MHU)**2/MHU**3*(B*(1.0-2.0*TAU-(1.0-TAU)*LOG(1.0-TAU))-LOG(1.0- & TAU))+((1.0-TAU)/2.0*(LOG(1.0-TAU))**2-(1.0-TAU)*LOG(1.0-TAU)+1.0- & TAU+ALPHA*(1.0-TAU-(1.0-TAU)*LOG(1.0-TAU))+ ALPHA**2*(1.0- & MHU)*TAU/(2.0*MHU)-(2+ALPHA-ALPHA/MHU))$$

! Third order calculation resulting from pertubation analysis

$$C1= -3.0/2.0*B**2-2.0*B+ALPHA**2/(2.0*MHU)*(1.0-1.0/MHU)$$

$$V3=A**3*((4.0-5.0*ALPHA/MHU-ALPHA**2/(2.0*MHU)+3.0*ALPHA**2/(2.0*MHU**2)) & *LOG(1.0-TAU)-0.5*B**2*1.0/(1.0-TAU)**2+(2.0*B+2.0*B**2-ALPHA**2/(2.0*MHU)+ &$$

$$\text{ALPHA}^{**2}/(2.0*\text{MHU}^{**2}))*1.0/(1.0-\text{TAU})-2.0*B*(\text{LOG}(1.0-\text{TAU}))^{**2}+0.5*(\text{LOG}(1.0-\text{TAU}))^{**3}-B*(\text{LOG}(1.0-\text{TAU}))/((1.0-\text{TAU})+C1)$$

$$U3=(V3*(V0-U0)+(V1-U1)*(V2-U2)-\text{MHU}^{**2}*U1*U2)/((V0-U0)+U0*\text{MHU}^{**2})$$

$$C2=(1.0+\text{MHU})^{**3}/\text{MHU}^{**4}*(-4.0-7.0/2.0*B^{**2}-7.0*B+9.0/2.0*\text{ALPHA}^{**2}/\text{MHU}-5.0*\text{ALPHA}-3.0*\text{ALPHA}^{**2}/2.0-\text{ALPHA}^{**3}/(2.0*\text{MHU}^{**2})*(1.0-\text{MHU})^{**2}+B^{**2}/2.0)$$

$$\begin{aligned} \text{PD3} = & -(1.0+\text{MHU})^{**3}/\text{MHU}^{**4}*((1.0-\text{TAU})*(-4.0-7.0/2.0*B^{**2}-7.0*B+9.0/2.0*\text{ALPHA}^{**2}/\text{MHU}- \\ & 5.0*\text{ALPHA}-3.0*\text{ALPHA}^{**2}/2.0-\text{ALPHA}^{**3}) \\ & + (1.0-\text{TAU})*\text{LOG}(1.0-\text{TAU})*(7.0/2.0+6.0*B+ \\ & +3.0*\text{ALPHA}*B+3.0*B^{**2}/2.0+\text{ALPHA}+3.0*\text{ALPHA}^{**2}/2.0)+B^{**2}/(2.0*(1.0-\text{TAU})) \& \\ & +(B+5.0/2.0*B^{**2}+\text{ALPHA}-3.0*\text{ALPHA}^{**2}/(2.0*\text{MHU})+1.0/2.0)*\text{LOG}(1.0-\text{TAU})+(1.0-\text{TAU}) \\ & *(\text{LOG}(1.0-\text{TAU}))^{**2}*(-2.0*B-3.0/2.0*(1.0+\text{ALPHA}))-B/2.0*(\text{LOG}(1.0-\text{TAU}))^{**2}+(1.0-\text{TAU}) \\ & /2.0*(\text{LOG}(1.0-\text{TAU}))^{**3}+C2 \end{aligned}$$

$$C3=((1+\text{MHU})/\text{MHU})^{**3}*(5.0/2.0+13.0/2.0*B^{**2}+5.0*B-5.0*\text{ALPHA}^{**2}/(2.0*\text{MHU})-\& \text{ALPHA}^{**3}/(2.0*\text{MHU}^{**3})*(\text{MHU}-1)^{**2})$$

$$\begin{aligned} \text{LAMDA3} = & ((1+\text{MHU})/\text{MHU})^{**3}*((-7.0*B/2.0)*(1.0-\text{TAU})*(\text{LOG}(1.0-\text{TAU}))^{**2}+(7.0*B^{**2}/2.0 - \\ & \text{ALPHA}^{**2}/(2.0*\text{MHU})+1.0/2.0)*\text{LOG}(1.0-\text{TAU}) -B/2.0*(\text{LOG}(1.0-\text{TAU}))^{**2} + (2.0+5.0*B+4*B^{**2}- \\ & 2*\text{ALPHA}^{**2}/\text{MHU})*(1.0-\text{TAU})*\text{LOG}(1.0-\text{TAU})+(-5.0/2.0-7.0*B^{**2} \\ & -5.0*B+5.0*\text{ALPHA}^{**2}/(2.0*\text{MHU})+\text{ALPHA}^{**3}/(2.0*\text{MHU}^{**3})*(\text{MHU}-1)^{**2}) \\ & *(1.0-\text{TAU})+B^{**2}/(2.0*(1.0-\text{TAU}))+ (1.0-\text{TAU})/2.0*(\text{LOG}(1.0-\text{TAU}))^{**3}+C3 \end{aligned}$$

! Summation of series for 1st order, 2nd order, and 3rd order pertubation solution

IF(ORDER.EQ.1)THEN

$$V=V0+\text{EPSI}*V1$$

$$U=U0+\text{EPSI}*U1$$

$$\text{LAMDA}=\text{LAMDA0}+\text{EPSI}*\text{LAMDA1}$$

$$\text{PD}=\text{PD0}+\text{EPSI}*\text{PD1}$$

ELSEIF(ORDER.EQ.2)THEN

$$V=V0+\text{EPSI}*V1+(\text{EPSI}^{**2})*V2$$

$$U=U0+\text{EPSI}*U1+(\text{EPSI}^{**2})*U2$$

$$\text{LAMDA}=\text{LAMDA0}+\text{EPSI}*\text{LAMDA1}+(\text{EPSI}^{**2})*\text{LAMDA2}$$

$$\text{PD}=\text{PD0}+\text{EPSI}*\text{PD1}+(\text{EPSI}^{**2})*\text{PD2}$$

ELSEIF(ORDER.EQ.3)THEN

$$V=V0+\text{EPSI}*V1+(\text{EPSI}^{**2})*V2+(\text{EPSI}^{**3})*V3$$

$$U=U0+\text{EPSI}*U1+(\text{EPSI}^{**2})*U2+(\text{EPSI}^{**3})*U3$$

$$\text{LAMDA}=\text{LAMDA0}+\text{EPSI}*\text{LAMDA1}+(\text{EPSI}^{**2})*\text{LAMDA2}+(\text{EPSI}^{**3})*\text{LAMDA3}$$

```

                PD=PD0+EPSI*PD1+(EPSI**2)*PD2+(EPSI**3)*PD3
            ENDIF

!           Converting normalized values into actual values

                VR=V*VI

                UP=U*VI

                P=PD*LO

                LI=LAMDA*LO

!           Penetration process stop conditions

! For RT > YP, the minimum rod velocity required to achieve penetration occurs when the penetration
! velocity is zero (UP = 0). At this point the target begins to behave as a rigid body and the rod
! bounces off the target.

                IF(RT.GT.YP.AND.VR.LE.SQRT(2.0*(RT-YP)/RHO_P))EXIT

! For RT < YP, the minimum rod velocity required to achieve penetration occurs when the penetration
! velocity is equal to the rod velocity (UP = VR). At this point the rod begins to behave as a
! rigid body.

                IF(RT.LT.YP.AND.VR.LE.SQRT(2.0*(YP-RT)/RHO_T))EXIT

! If the penetration is greater than the thickness of the target, perforation is achieved terminate
! loop

                IF(P.GT.THK)EXIT

! If the instantaneous length is less than zero, then the rod had totally eroded, Terminate Loop

                IF(LI.LT.0.0)EXIT

! Output data for graphical processing

                WRITE(12, 100), T, VR, UP, P, LI

100           FORMAT(F10.7, 5X, F15.10, 5X, F15.10, 5X, F10.8, 5X, F10.8)

! Time increment, 1 microsecond step size

                T=T+0.000001

            END DO

            PRINT*, EPSI

            END PROGRAM Pertubation

```

1 DEFENSE TECHNICAL  
(PDF INFORMATION CTR  
ONLY) DTIC OCA  
8725 JOHN J KINGMAN RD  
STE 0944  
FORT BELVOIR VA 22060-6218

1 US ARMY RSRCH DEV &  
ENGRG CMD  
SYSTEMS OF SYSTEMS  
INTEGRATION  
AMSRD SS T  
6000 6TH ST STE 100  
FORT BELVOIR VA 22060-5608

1 INST FOR ADVNCD TCHNLGY  
THE UNIV OF TEXAS  
AT AUSTIN  
3925 W BRAKER LN  
AUSTIN TX 78759-5316

1 DIRECTOR  
US ARMY RESEARCH LAB  
IMNE ALC IMS  
2800 POWDER MILL RD  
ADELPHI MD 20783-1197

3 DIRECTOR  
US ARMY RESEARCH LAB  
AMSRD ARL CI OK TL  
2800 POWDER MILL RD  
ADELPHI MD 20783-1197

3 DIRECTOR  
US ARMY RESEARCH LAB  
AMSRD ARL CS IS T  
2800 POWDER MILL RD  
ADELPHI MD 20783-1197

ABERDEEN PROVING GROUND

1 DIR USARL  
AMSRD ARL CI OK TP (BLDG 4600)

NO. OF  
COPIES ORGANIZATION

2 INST FOR ADVNCD TECH  
S BLESS  
H FAN  
4030-2 W BRAKER LN  
AUSTIN TX 78759

3 CDR US ARMY ARDEC  
AMSRD AAR AEE W  
E BAKER  
A DANIELS  
R FONG  
B3022  
PICATINNY ARSENAL NJ 07806-5000

3 CDR US ARMY RSCH OFC  
S DAVIS  
K IYER  
A RAJENDRAN  
PO BOX 12211  
RSCH TRIANGLE PK NC 27709-2211

1 CDR NAVAL SURF WARFARE CTR  
DAHLGREN DIVISION  
W HOYE G02  
17320 DAHLGREN RD  
DAHLGREN VA 22448-5100

2 CDR NAVAL SURF WARFARE CTR  
DAHLGREN DIVISION  
T SPIVAK G22  
F ZERILLI  
17320 DAHLGREN RD  
DAHLGREN VA 22448-5100

1 AIR FORCE ARMAMENT LAB  
AFATL DLJR  
D LAMBERT  
EGLIN AFB FL 32542-6810

2 DARPA  
W SNOWDEN  
S WAX  
3701 N FAIRFAX DR  
ARLINGTON VA 22203-1714

2 LOS ALAMOS NATL LAB  
P HOWE MS P915  
PO BOX 1663  
LOS ALAMOS NM 87545

NO. OF  
COPIES ORGANIZATION

1 LOS ALAMOS NATL LAB  
L HULL MS A133  
PO BOX 1663  
LOS ALAMOS NM 87545

5 SANDIA NATL LAB  
R BELL MS0836 9116  
D CRAWFORD MS0836 9116  
E HERTEL MS0836 9116  
S SILLING MS0820 9232  
D PRECE MS 0819  
ALBUQUERQUE NM 87185-0100

3 DIR LAWRENCE LIVERMORE  
NATL LAB  
D BAUM L099  
M MURPHY  
C SIMONSON MS  
PO BOX 808 MS L35  
LIVERMORE CA 94550

2 SOUTHWEST RSCH INST  
C ANDERSON  
J WALKER  
PO DRAWER 28510  
SAN ANTONIO TX 78228-0510

2 CDR US ARMY AVN & MISSILE CMD  
AMSAM RD PS WF  
S CORNELIUS  
S HOWARD  
REDSTONE ARSENAL AL 35898-5247

2 AEROJET  
J CARLEONE  
S KEY  
PO BOX 13222  
SACRAMENTO CA 95813-6000

1 CMPTNL MECHS CNSLTNTS  
J ZUKAS  
PO BOX 11314  
BALTIMORE MD 21239-0314

3 DETK  
R CICCARELLI  
W FLIS  
M MAJERUS  
3620 HORIZON DR  
KING OF PRUSSIA PA 19406

<u>NO. OF COPIES</u>	<u>ORGANIZATION</u>
1	TEXTRON DEFENSE SYSTEMS C MILLER 201 LOWELL ST WILMINGTON MA 01887-4113
1	D R KENNEDY & ASSOC INC D KENNEDY PO BOX 4003 MOUNTAIN VIEW CA 94040
1	LOCKHEED MARTIN ELECTRONICS & MISSILES G BROOKS 5600 SAND LAKE RD MP 544 ORLANDO FL 32819-8907
4	GD OTS C ENGLISH T GRAHAM D MATUSKA J OSBORN 4565 COMMERCIAL DR A NICEVILLE FL 32578
2	GD OTS D BOEKA N OUYE 2950 MERCED ST STE 131 SAN LEANDRO CA 94577-0205
1	ZERNOW TECHNICAL SVS INC L ZERNOW 425 W BONITA AVE STE 208 SAN DIMAS CA 91773
1	PM JAVELIN PO SSAE FS AM EG C ALLEN REDSTONE ARSENAL AL 35898-5720
1	PM TOW SFAE TS TO J BIER REDSTONE ARSENAL AL 35898-5720
1	HALLIBURTON ENERGY SVCS JET RESEARCH CENTER D LEIDEL PO BOX 327 ALVARADO TX 76009-9775

<u>NO. OF COPIES</u>	<u>ORGANIZATION</u>
1	NORTHROP GRUMMAN DR D PILLASCH B57 D3700 PO BOX 296 1100 W HOLLYVALE ST AZUSA CA 91702
1	INTRNTL RSRCH ASSOC D ORPHAL 4450 BLACK AVE PLEASANTON CA 94566-6105
1	TELEDYNE RISI INC J VAROSH PO BOX 359 TRACY CA 95378
	<u>ABERDEEN PROVING GROUND</u>
48	USARL AMSRD ARL WM J SMITH AMSRD ARL WM EG E SCHMIDT AMSRD ARL WM MB W DEROSSET R DOWDING AMSRD ARL WM T B BURNS AMSRD ARL WM TA W GILLICH W GOOCH M BURKINS T HAVEL M KEELE D KLEPONIS J RUNYEON S SCHOENFELD AMSRD ARL WM TB P BAKER R BANTON R LOTTERO J STARKENBERG AMSRD ARL WM TC G BOYCE R COATES T FARRAND E KENNEDY K KIMSEY L MAGNESS S SCHRAML D SCHEFFLER B SORENSEN

NO. OF  
COPIES ORGANIZATION

R SUMMERS  
C WILLIAMS (6 CPS)  
W WALTERS (6 CPS)  
R ANDERSON  
M FERMEN-COKER  
AMSRD ARL WM TD  
Y HUANG  
T WEERASOORIYA  
T W BJERKE  
E RAPACKI  
S SEGLETES  
M RAFTENBERG  
AMSRD ARL SL BE  
A PRAKASH

INTENTIONALLY LEFT BLANK.